A COLUMN BASED VARIANCE ANALYSIS APPROACH TO STATIC RESERVOIR MODEL UPGRIDDING

A Thesis

by

MATTHEW BRANDON TALBERT

Submitted to the Office of Graduate Studies of
Texas A&M University
in partial fulfillment of the requirements for the degree of

MASTER OF SCIENCE

August 2008

Major Subject: Petroleum Engineering

A COLUMN BASED VARIANCE ANALYSIS APPROACH TO STATIC RESERVOIR MODEL UPGRIDDING

A Thesis

by

MATTHEW BRANDON TALBERT

Submitted to the Office of Graduate Studies of
Texas A&M University
in partial fulfillment of the requirements for the degree of

MASTER OF SCIENCE

Approved by:

Chair of Committee,	Akhil Datta-Gupta
Committee Members,	Yalchin R. Efendiev
	Robert A. Wattenbarger
Head of Department,	Stephen A. Holditch

August 2008

Major Subject: Petroleum Engineering

ABSTRACT

A Column Based Variance Analysis Approach to

Static Reservoir Model Upgridding. (August 2008)

Matthew Brandon Talbert, B.S., Texas A&M University

Chair of Advisory Committee: Dr. Akhil Datta-Gupta

The development of coarsened reservoir simulation models from high resolution geologic models is a critical step in a simulation study. The optimal coarsening sequence becomes particularly challenging in a fluvial channel environment where the channel sinuosity and orientation can result in pay/non-pay juxtaposition in many regions of the geologic model. The optimal coarsening sequence is also challenging in tight gas sandstones where sharp changes between sandstone and shale beds are predominant and maintaining the pay/non-pay distinction is difficult. Under such conditions, a uniform coarsening will result in mixing of pay and non-pay zones and will likely result in geologically unrealistic simulation models which create erroneous performance predictions. In particular, the upgridding algorithm must keep pay and non-pay zones distinct through a non-uniform coarsening of the geologic model.

We present a coarsening algorithm to determine an optimal reservoir simulation grid by grouping fine scale geologic model cells into effective simulation cells. Our algorithm groups the layers in such a way that the heterogeneity measure of an appropriately defined static property is minimized within the layers and maximized

between the layers. The optimal number of layers is then selected based on an analysis resulting in a minimum loss of heterogeneity.

We demonstrate the validity of the optimal gridding by applying our method to a history matched waterflood in a structurally complex and faulted offshore turbiditic oil reservoir. The field is located in a prolific hydrocarbon basin offshore South America. More than 10 years of production data from up to 8 producing wells are available for history matching. We demonstrate that any coarsening beyond the degree indicated by our analysis overly homogenizes the properties on the simulation grid and alters the reservoir response. An application to a tight gas sandstone developed by Schlumberger DCS is also used in our verification of our algorithm. The specific details of the tight gas reservoir are confidential to Schlumberger's client. Through the use of a reservoir section we demonstrate the effectiveness of our algorithm by visually comparing the reservoir properties to a Schlumberger fine scale model.

DEDICATION

I dedicate this work to God.

I also dedicate this work to my family for their love and support. To my mother and father I appreciate the encouragement and the examples that you have provided in my life that allow me to accomplish my dreams and ambitions with integrity and honest work. I also appreciate your guidance in my religious development and support in the rough times of my life. To Chris and Whitney, I thank you for the support and friendship that has never wavered and provided strength in pursuit of my dreams. To John, I pray that all your dreams are reached and that your compassion, dedication, intellectual curiosity, and pursuit of justice be comparable to your parents, some of the greatest people I know.

ACKNOWLEDGEMENTS

I would like to thank my graduate advisor, Dr. Akhil Datta-Gupta, for his guidance in my research and educational development. To the members of my graduate committee, Dr. Robert Wattenbarger, and Dr. Yalchin Efendiev, I would like to offer deep gratitude for their contributions to my education and for their guidance. I would also like to thank Dr. Maria Barrufet for her time and effort. I acknowledge Chevron Energy Technology Company for the experience and opportunity to obtain an advanced degree, one of my career objectives. I would also like to thank both Dr. Xianlin Ma and Dr. Adedayo Oyerinde for their friendship and guidance in the completion of my research. To everyone in rooms 701 and 702 I thank you for your friendship and encouragement.

TABLE OF CONTENTS

Page

LIST OF FIGURES

FIGURE Page

FIGURE Page

LIST OF TABLES

1. INTRODUCTION

1.1 Literature Review

The process of upscaling is an active area of research due to the increasingly complex earth models that are being developed for reservoir management. Increasing computer power has led to higher resolution geologic models (Durlofsky et. al 1996; Li and Beckner 2000; Gorell and Bassett 2001; Chawathé and Taggart 2004; Fincham et. al 2004; King et al. 2006; Wang et. al 2005; Nair and Al-Maraghi 2006; Zhang et. al 2006). Many methods and ideas have been presented in the literature ranging from flow based to static upscaling methods. The purpose of upscaling reservoir models is to reduce the computational cost associated with flow simulation and at the same time maintain an accurate reservoir response. A natural first step in upscaling is upgridding of the original earth model for simulation (Durlofsky et. al 1996; Kumar et. al 1997; Li and Beckner 2000; Chawathé and Taggart 2004; King et. al 2006). Once upgridding is completed the next step is to reassign the reservoir properties to the simulation grid using various property upscaling methods (Durlofsky et. al 1996; Kumar et. al 1997; Chawathé and Taggart 2004; Fincham et. al 2004).

Reservoir engineering has accepted simulation as a valid tool for reservoir management (Milliken et. al 2008). Traditional studies as well as fit for purpose models are now being used to determine the optimal course of action which maximizes performance and profit. Traditional models are built in a deterministic workflow that is

---

This thesis follows the style of *SPE Journal*.

used to predict reservoir recovery (Gorell and Bassett 2001). Both traditional and fit for purpose models, which are built to determine the range of uncertainty in a model, need to be upscaled to efficiently be used as a reservoir engineering resource. Fit for purpose models are usually a fraction of the full field and are used to rapidly asses how variation in input parameters affects the reservoir response (Gorell and Bassett 2001). A common method in the geological and simulation community of arriving at a reservoir simulation model is to statistically generate several fines scale models, upscale the models and then perform flow simulations on each to determine which model approaches the historical data for the field (Sablok and Aziz 2005).

Innovations in computer technology including clustering, parallel processors, and increased CPU performance have not closed the gap between the ability of geoscientists to develop models and engineers to simulate the physics of fluid flow (Li and Beckner 2000; Gorell and Bassett 2001; Wang et. al 2005; Milliken et. al 2008). At present serial reservoir finite difference simulation can handle on the high end of the scale approximately 500,000 active gridblocks while models are being built at approximately 50,000,000 gridblocks on the high end of the scale (Gorell and Bassett 2001).

The process of upscaling was studied in the 10th SPE Comparative Solution Project which involved nine participating companies (Christie and Blunt 2001). This comparative solution project provided participants with two test cases to determine how well the industry is upscaling reservoirs for use in simulation studies. The first test case is a simple 2D model that could easily be simulated on the full field scale. The second test case is a difficult 3D reservoir model that is very difficult to simulate on the full

field scale. The results showed a wide range of coarse simulation grid sizes. The majority of companies used flow based methods and relative permeability alterations to perform the upscaling (Christie and Blunt 2001). The comparative solution showed that there is no standard methodology currently used in the industry to upscale reservoirs. This study did find that no-flow boundaries are better than open boundary conditions in local upscaling calculations (Fincham et. al 2004).

Varying ideas on the process of upscaling reservoir simulation models have been presented. There are three base methods of upgridding a reservoir. The first method uses static properties to determine an objective function. The objective function is used in an optimization algorithm which determines the coarse grid number of layers that accurately simulates the fine grid model. The next method of upscaling is flow-based optimization. Flow based methods require the solution of flow equations to determine the flux through each gridblock. The last method and the least technically based is a visual interpretation and grouping (Kumar et. al 1997). Once the model has been upgridded using one of the base methods, the reservoir properties are upscaled to apply on the new coarse model. The process of upgridding and upscaling models removes outliers in the reservoir properties therefore removing unusually large or small values and ultimately narrowing the range (Qi and Hesketh 2004).

There are many types of classifications that can be used when identifying the type of upscaling to be applied to reservoir properties after upgridding a model as outlined by Sablok and Aziz (2005). The majority of the current work in upscaling has focused on single-phase upscaling, multiphase upscaling, local solution based grids, and global

solution based grids. Single-phase upscaling and multiphase upscaling refer to how the reservoir parameters are being upscaled. The term single-phase upscaling refers to a model in which only the absolute permeability is upscaled for the coarse grid neglecting relative permeability and capillary pressure which are accounted for in the multiphase upscaling techniques. Local and global solution based methods refer to the scale upon which the reservoir parameters are calculated (Sablok and Aziz 2005; Wu et. al 2007). The global scale-up method is generally more accurate than local methods however they are more costly (Wu et. al 2007).

The flow based methods are computationally time-consuming and can alter on the solution based upon boundary conditions used in determining the flux (Stern and Dawson 1999; Efendiev and Durlofsky 2004; Zhang et. al 2006; Wu et. al 2007). The flow based method relies on a solution of the pressure equation for each cell to determine the amount of flux through the gridblock. Using the information obtained through fluxes we can group layers that have a low amount of flow while maintaining the layers with high levels of flow separate to maintain the areas of higher relevance (Fincham et. al 2004). The flow equation requires that a boundary condition be placed either using local or global boundary conditions. The application of incorrect boundary conditions is often a problem in localized upscaling. The types of boundary conditions include no-flow, constant pressure, linear pressure, and periodic functions which often do not accurately recreate the reservoirs boundary conditions (Zhang et. al 2006). The problem of boundary conditions has been addressed by many authors with varying approaches. An approach that incorporates wells and actual reservoir boundary

conditions including faults has been developed that maintains dominant flow paths (Zhang et. al 2006). This method requires a single phase pressure solution and alteration of the relative permeability's in the merged layers. Stern and Dawson (1999) proposed a method that uses single phase breakthrough times and differences between coarse and fine scale fluxes as the objective functions in their layer optimization method. Stern and Dawson's method sequentially coarsens a fine scale model but requires a sweep efficiency calculation after each merging to determine the appropriate number of layers to represent the fine scale model.

Static based methods use reservoir properties to create a new property that is used to optimize the model layering. Statistical optimization was first used by Testerman (1962) for well-zonation. The model started with a single layer (wellbore) and sequentially added layers into the model until a predetermined level of heterogeneity was achieved (Testerman 1962). Li and Beckner (2000) applied Testerman's approach to create a method that uses porosity, permeability, and facies as the static property for reservoir model layering optimization. This static property combines both the geological and engineering important parameters into our optimization parameter. This is the same property that we use in our approach. We differ in our algorithm by using columnar averages to calculate variance and use sequential coarsening instead of refinement (King et. al 2006). Li and Beckner's (2000) method requires creation of a residual curve in which engineers judgment is required to determine the optimal layers.

The method we are using has been previously used in a streamline simulation formulation. Osako and Datta-Gupta (2007) used a variation of our static parameter to

perform min-max optimization in determining what layers to group based upon ‘slowness’. This work has previously validated our algorithm and provided a basis for our approach to determining the optimal number of layers. Streamlines have also been used in conjunction with a minimization algorithm to determine the appropriate number of layers in a model (Nair and Al-Maraghi 2006). This is a hybrid approach that uses both the minimization features as well flux calculations, therefore combining the static and flow based algorithms.

1.2 Objectives of the study

The objectives of the study are split into two parts. The first part is a development of a C++ software package of our algorithm that minimizes variance removed while maintaining the maximum variance in the model. The software will be able to operate on both gas and oil reservoirs with minimal user interaction. The software also will be applicable to both layered and non-layered reservoirs.

The second part of the research is applications to both a channelized reservoir and a tight gas sandstone reservoir. The reservoir response and visual comparison to coarse grid models is used as measure of the applicability of our algorithm and validation of our technique.

1.3 Thesis Outline

We first discuss the mathematical development and approach we used in development of our algorithm. The Buckley-Leverett theory is also discussed as it is a significant portion of our algorithm in the oil reservoir option.

Next we apply the algorithm to a synthetic case to test our procedure. The test case is a 2D reservoir and results are compared to a uniform upgridding on a visual grid analysis and time of flight comparison.

The algorithm is then applied on a 3D channelized reservoir. The results are compared to a full field simulation using both field and well responses. The water saturation versus time is used as another comparison to the fine scale model. As a final validation of our algorithm we perform a uniform upgridding on the reservoir model and compare the well responses.

Finally we apply our algorithm to a tight gas reservoir. The case is confidential from Schlumberger DCS and we visually investigate how our algorithm has merged both the pure statistical optimization and layer based optimization grids. We compare the resulting grids with the original fine scale model.

2. MATHEMATICAL FORMULATION AND APPROACH

2.1 Variance Analysis

The first part of our algorithm determines which two adjacent layers are to be merged. This is based on an analysis of the total variation of a defined static property denoted as p. In oil reservoirs, we choose the property given by $p = \frac{f'k}{\phi}$ where $\frac{k}{\phi}$ is the interstitial velocity and the Buckley-Leverett speed, f', includes the facies and saturation dependent relative permeability terms (King et. al 2006). In gas reservoir analysis we use a revised static property, p, which does not include the Buckley-Leverett speed. The new property is defined as $p = \frac{k}{\phi}$. In both oil and gas reservoirs we assume a two-phase system. In the oil reservoir case the second phase is water. In gas reservoirs we assume the second phase is water at irreducible water saturation, s_{wirr}, therefore the total permeability can be used in our static property or the user has provided the effective gas permeability. The total variation, our measure of heterogeneity during coarsening, is decomposed into within cell variance (W) and between cell variance (B). Following King et al. (2006), these quantities are given by the following expressions:

$$B = \sum_{x,y,z=1}^{NX,NY,NZ} n_{x,y,z}\left(p^{C}_{x,y,z} - \overline{p}_{x,y} \right)^2 \tag{2.1}$$

Equation 2.1 is a summation of the reservoir model that is equivalent to the variation preserved in the model after upgridding. One of the goals of our algorithm is to

maximize the variation preserved in our model and also preserve the geological markers during upgridding.

$$W = \sum_{x,y,z=1}^{NX,NY,NZ} n_{x,y,z}\left(p_{x,y,z} - p^{C}_{x,y,z}\right)^2 \tag{2.2}$$

Equation 2.2 is the method of determining the amount of variation removed from the model after each layer is merged in our algorithm. Another goal of our algorithm is to minimize the amount of variation removed from our model. The summation of our goals creates a min-max objective for our algorithm to satisfy.

$$p^{C}_{x,y,z} = \sum_{z} n_{x,y,z} \cdot p_{x,y,z} \Big/ \sum_{z} n_{x,y,z} \tag{2.3}$$

Equation 2.3 is the transitional static property that is calculated after each merging in our algorithm. This transitional property is used to determine the amount of the heterogeneity removed and the amount preserved during iterations in the program by applying the value into equation 2.1 and equation 2.2.

$$\overline{p}_{x,y} = \sum_{z=1}^{NZ} n_{x,y,z} \cdot p_{x,y,z} \Big/ \sum_{z=1}^{NZ} n_{x,y,z} \tag{2.4}$$

Equation 2.4 is the column based average of our fine scale static property used for determination of variation. A weight based average is used in all our variance calculations with the property *n* being equal to the bulk volume of each cell.

The within cell variation (W) quantifies the amount of heterogeneity lost during the coarsening whereas between the cell variation (B) quantifies the amount of heterogeneity

preserved. The total variation which is the overall measure of heterogeneity is given by equation 2.5.

$$H = W + B \tag{2.5}$$

Figure 1 shows the trends of W and B as a function of number of model layers. The optimal number of layers will be decided by minimizing W (that is minimizing the loss of heterogeneity) or alternately maximizing B (that is preserving the geologic heterogeneity to the maximum possible extent). In figure 1 the within cell variation (W) shows three heterogeneity regimes: a slow increase for large number of layers, a rapid increase for few layers, and a moderate increase between the two. The optimal number of layers should be in the intermediate regime transitioning from the slow increase to the rapid increase in heterogeneity removed from the model. The major steps of our upgridding approach are as follows:

Step 1: Calculate the property p based on permeability, porosity and relative permeability at each grid cell.

Step 2: Group two adjacent layers sequentially and calculate the 'within the cell variation (W)' to quantify the loss of heterogeneity from the merging.

Step 3: Merge those two layers that result in minimal loss in heterogeneity based on the calculations in step 2.

Step 4: Repeat steps 2 through 3 and continue merging layers until the model is reduced to two layers.

Step 5: Determine the optimal number of layers from the plot of 'W' vs. number of layers.

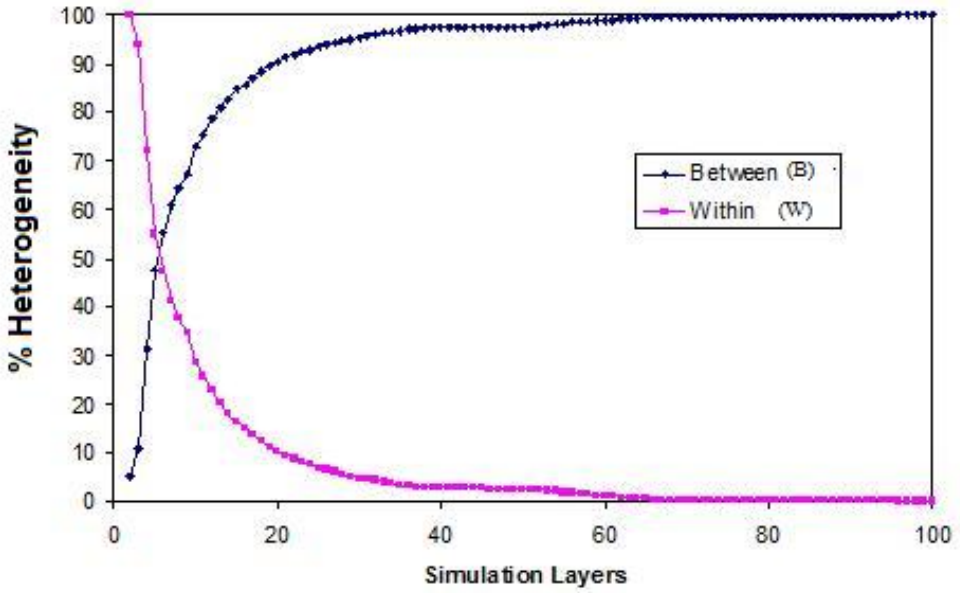

Figure 1 - Between-Within heterogeneity analysis.

2.2 Buckley-Leverett

Our algorithm uses the Buckley-Leverett theory of frontal displacement for oil reservoirs. This method applies each specific rock type in our reservoir with the relative rock speed which is then used in our variance analysis.

The fractional water is calculated using equation 3.1 (Dake 1978). There are several assumptions in our Buckley-Leverett that we use in our algorithm. These include a negligible capillary pressure gradient and horizontal flow. This reduces the fractional flow formula to be reduced to equation 3.2 (Buckley and Leverett 1942; Dake 1978). For each rock type a fractional flow versus water saturation curve is produced through chord slope enhanced relative permeability tables. After the fractional flow curves are created our algorithm searches through the stored data and saturation points to create slopes from the information. The slopes initial point is always the irreducible water saturation.

Once the vector of slopes are created for each rock type our algorithm searches through the stored slopes to determine a maximum which is equivalent to the saturation frontal speed as shown in equation 3.3 (Buckley and Leverett 1942; Dake 1978). Figure 2 shows a fractional flow curve that was created using our algorithm after chord slope enhancement for an unfavorable mobility ratio and the associated maximum slope.

$$f_w = \frac{1+0.001127\frac{kk_{ro}\,A}{\mu_o\ q_t}\left[\frac{\partial P_C}{\partial L}-0.433\Delta psin(\alpha)\right]}{1+\frac{k_{ro}*\mu_w}{k_{rw}*\mu_o}} \tag{3.1}$$

$$f_w = \frac{1}{\left(1+\frac{k_{ro}*\mu_w}{k_{rw}*\mu_o}\right)} \tag{3.2}$$

$$v = \frac{q_i df_w}{A\phi dS_W} \tag{3.3}$$

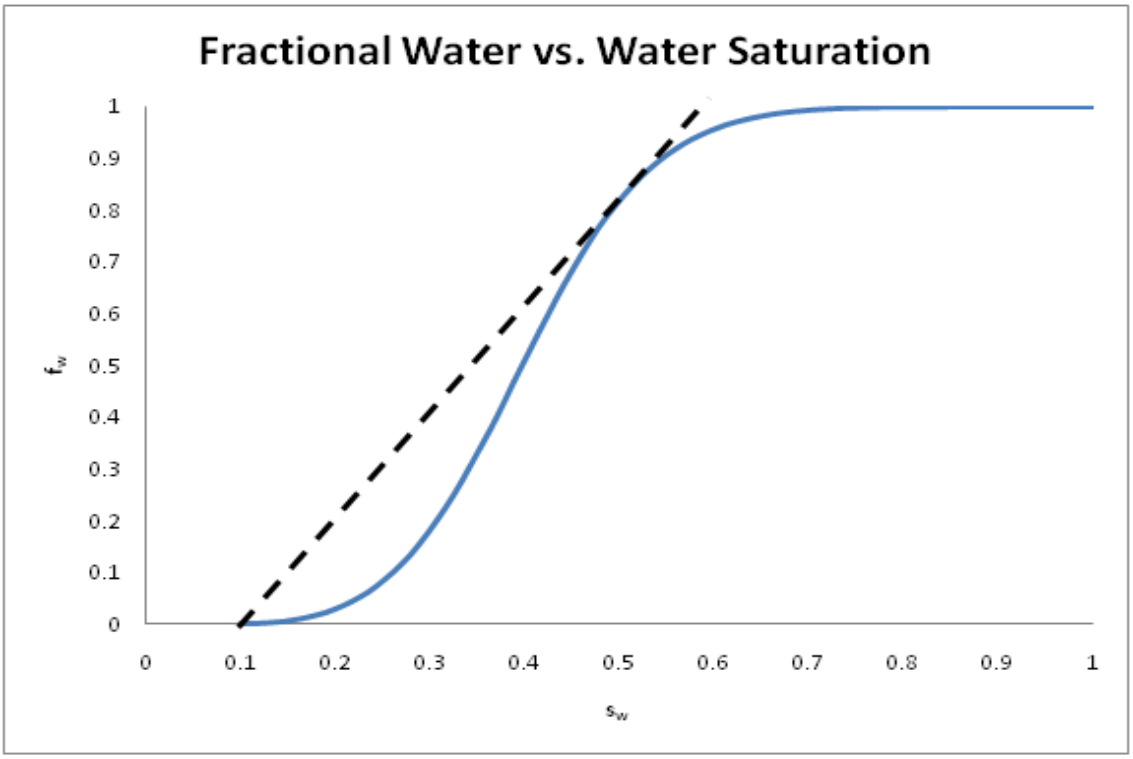

Figure 2 – Fractional flow curve.

3. SYNTHETIC EXAMPLE

We illustrate our procedure using a simple synthetic example. A 2D channel on a 100x100 cross section is used to demonstrate our approach and compare the results with a uniform coarsening method. To simplify the problem, the property upscaling is performed with arithmetic averaging. The fine scale model is shown in figure 3. In figure 4 we have shown the percentage of heterogeneity as quantified by 'between the cell variation (B)' vs. the number of layers. Also superimposed is a curve that shows the optimal number of layers as given by the point of inflection in the 'B' curve. The results show 18 layers as the optimal, which preserves 88% of the fine model heterogeneity. The same results can also be arrived at by using the 'within the cell variation (W)' as outlined in the step-by-step procedure above. Figure 5 shows the channels described by 18 layers using our optimal upgridding algorithm, and figure 6 gives the channels described by 20 layers using the uniform upgridding method. Compared to the fine scale, the first channel is clearly smeared and distorted by the uniform upgridding. However, our upgridding method appears to have preserved the channel geometry. Next, we analyze the layer models using streamlines. An injector is introduced on the left of the cross-section and a producer on the right. Minimum values in the time of flight characterize the channels in our model. The inverse time of flight distribution is shown in figure 7. There are two peaks which correspond to the two channels. It is clear from the comparison that the 18 layer optimal upgridding solution is closer to the fine scale model than the 20 layer uniform upgridding solution.

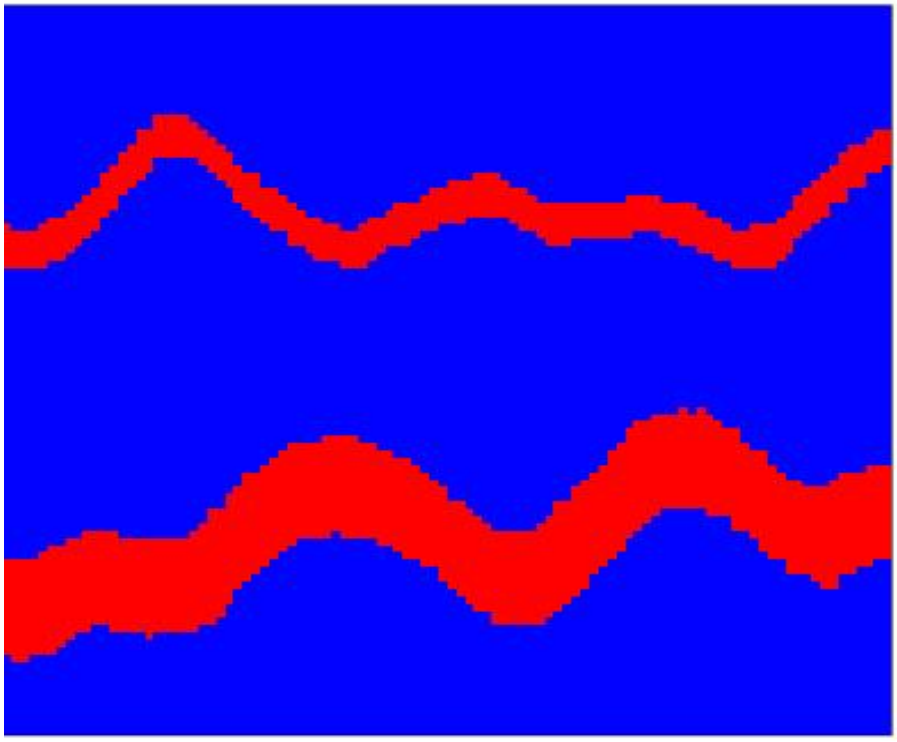

Figure 3 - 2D fine scale synthetic model.

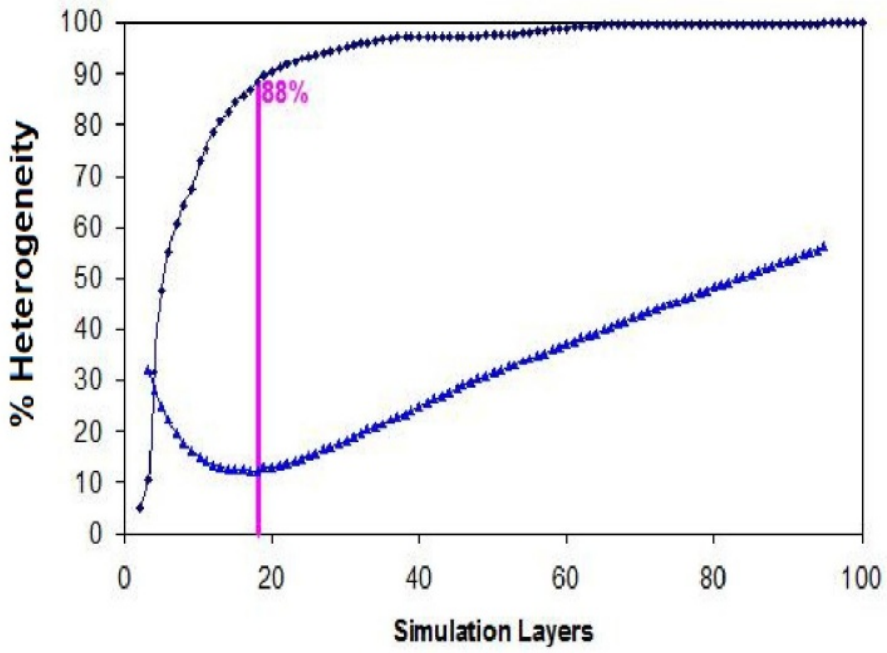

Figure 4 - Between-layer variance analysis.

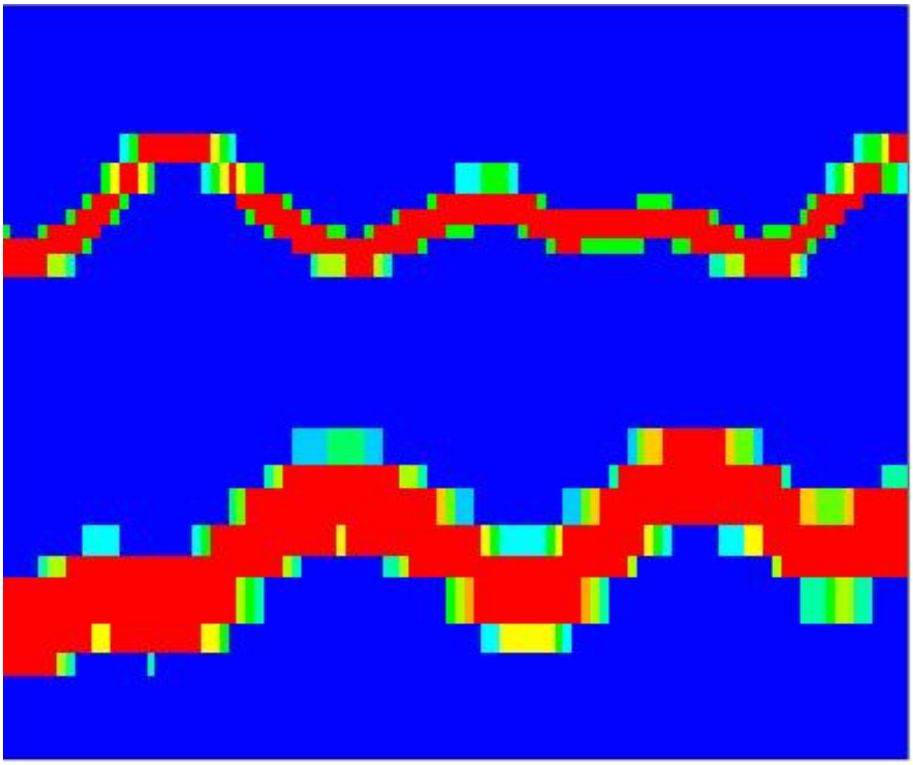

Figure 5 – 18 layer optimal synthetic model using variance analysis.

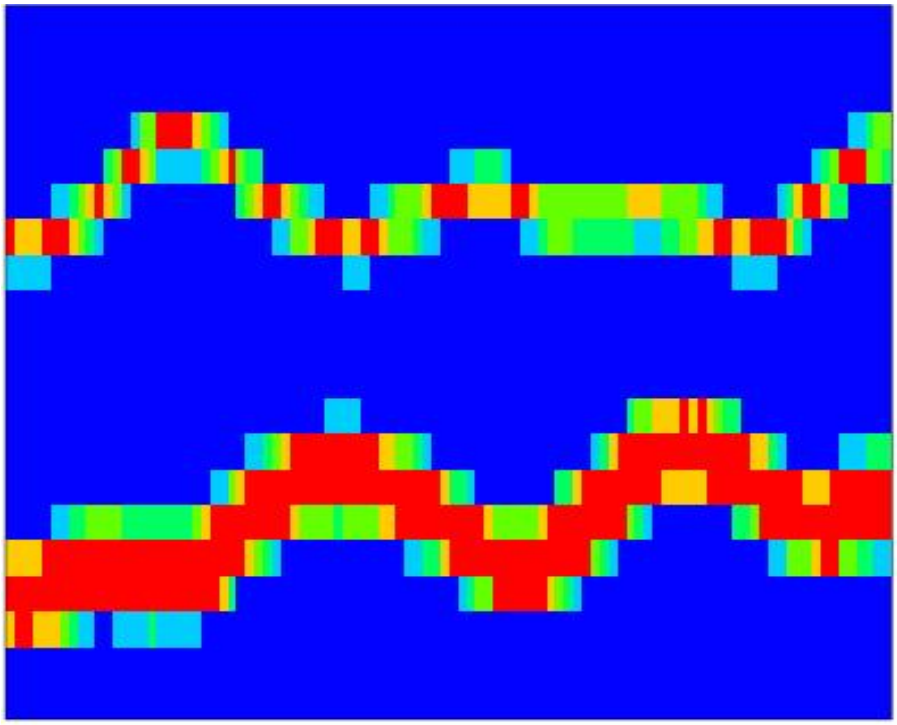

Figure 6 - 20 layer synthetic model using uniform upgridding.

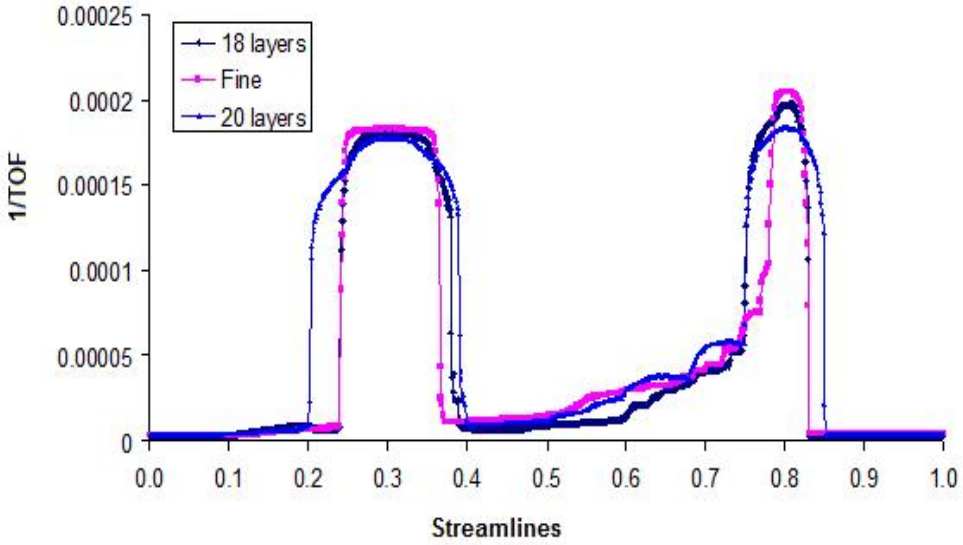

Figure 7 - Distribution of inverse time of flight.

4. 3D CHANNELIZED RESERVOIR CASE STUDY

4.1 Reservoir Description

A South American offshore Eocene reservoir that is composed of sheet and channel sands is used to demonstrate our algorithm (Hohl et. al 2006). The sands are divided into 3 distinctive regions, Sand A, Sand B, and the Main Sand, all with a k_v/k_h ratio of 0.01. The field was initially produced under primary depletion with 2 producers using well productivity and water cut as the tools for monitoring. Eventually the field was converted to a waterflood through 3 years of field workovers adding 6 producers and 4 injectors. The field has a total 8 producer and 4 injector wells for use in history matching and forecasting in our simulation. The reservoir model was developed as an 81 layer structurally complex and faulted turbiditic oil reservoir with excellent quality sands with high permeability, excellent porosity and distinctive transitions between low and high quality sands (Hohl et. al 2006). The wells are controlled on oil targets as the primary constraint and the secondary constraint is a minimum bottomhole pressure. Table 1 shows the well constraints that are used in our simulation of the channelized reservoir.

Table 1 – Well Producing Constraints.

Well Name	Oil Rate Target	BHP Limit (psi)
BJ_U	7988	1000
BJ_V	852	1000
BJ_Q	11027	1000

Figure 8 shows the 3D perspective view of the 81 layer model. The channels are visible as higher permeability streaks in the figure. Figure 9 through figure 11 shows the Sand A, Sand B, and Main Sand permeability distribution respectively. It is evident that the reservoir becomes more highly channelized moving down towards the Main Sand. The Sand A has a fairly smeared permeability distribution and Sand B has a tighter definition of channels in the reservoir. Moving to the Main Sand we see that there are highly channelized permeability features in the reservoir.

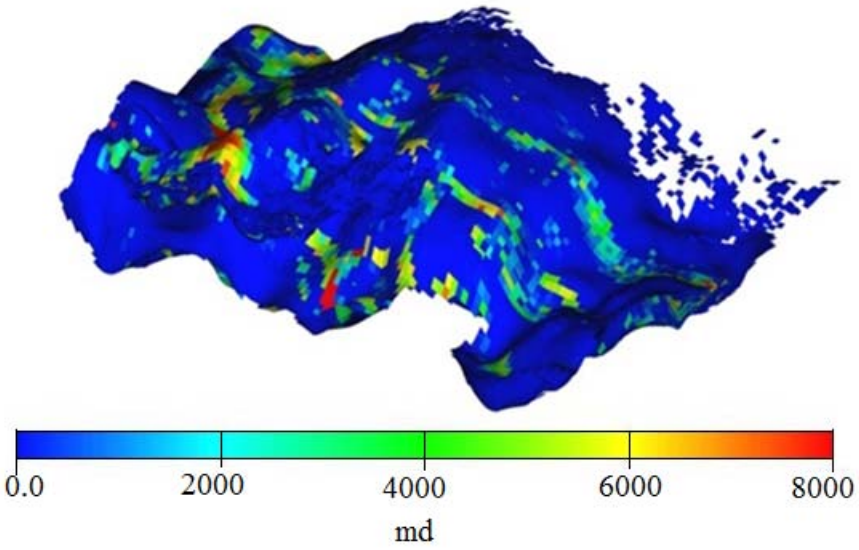

Figure 8 - 81 layer, 3D model permeability distribution.

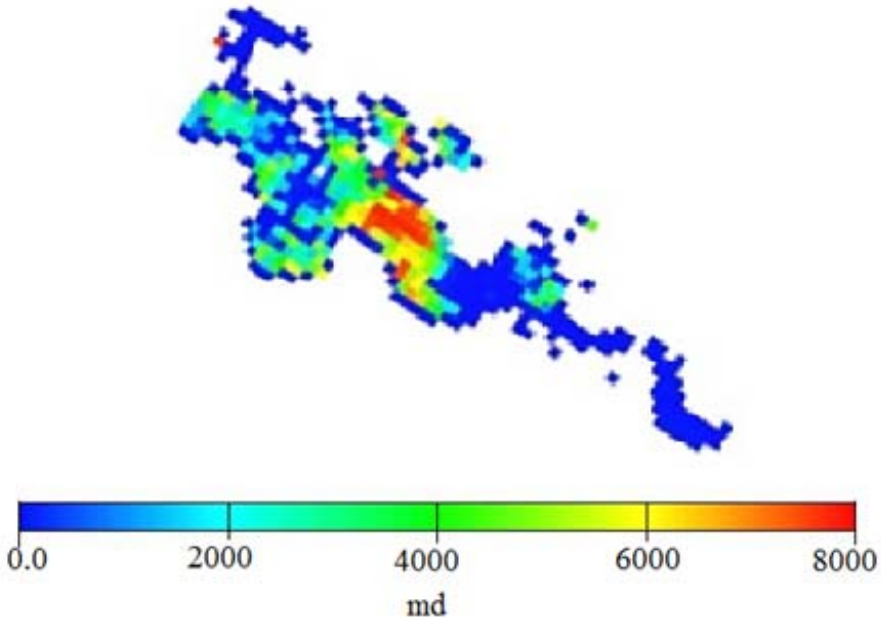

Figure 9 - 81 layer model, Sand A permeability distribution.

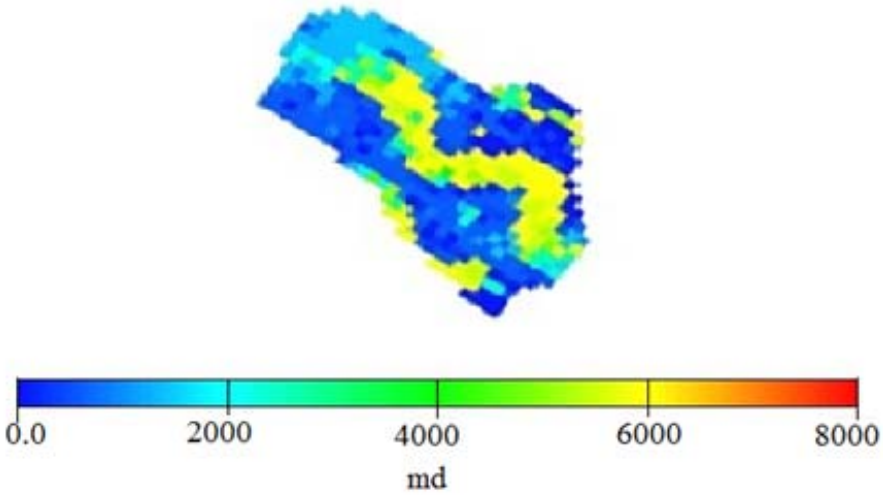

Figure 10 - 81 layer model, Sand B permeability distribution.

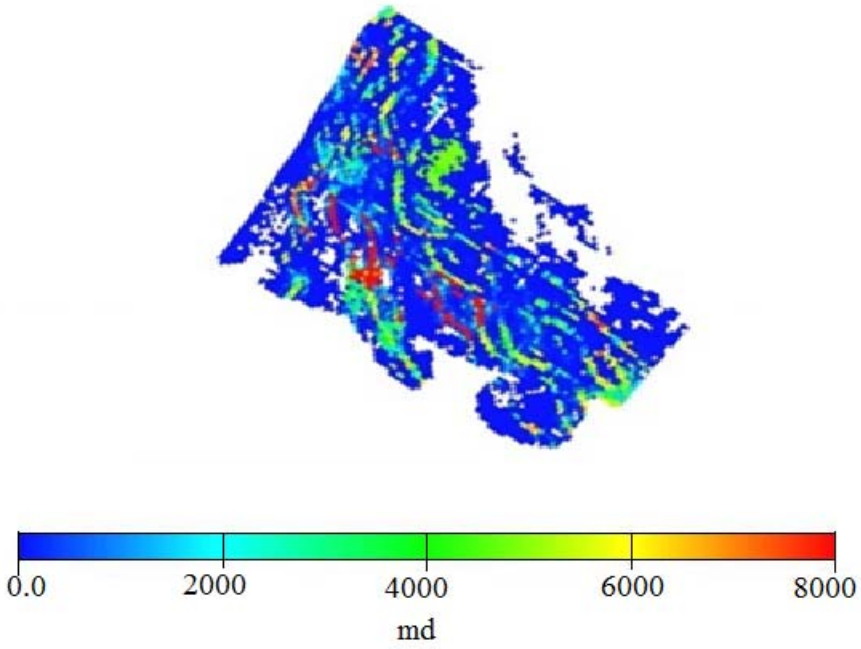

Figure 11 - 81 layer model, Main Sand permeability distribution.

4.2 Upgridding Analysis

We have applied the upgridding algorithm to a fine scale 81 layer model. Figure 12, shows the normalized 'within cell variation (W)' as a function of the number of layers. Recall that W quantifies the loss of heterogeneity as a result of layer grouping. Clearly, the curve shows a distinct upward trend below about 30 layers. In fact, below 36 layers, the layers across the geologic markers are merged. To avoid this, we chose 36 layers as the optimal in this case. We have also applied our layer based optimization analysis to this case and using the R statistical script have arrived again at 36 layers as shown in figure 13. However, if the optimal number of layers is chosen based on the inflection point in the pure statistical R analysis curve we arrive at 26 layers as shown in figure 14.

The inflection is determined by analyzing the relationship between the within cell variance and simulation layers as shown in figure 1. Two linear regressions were fit on the two sides of the curve, and then the weighted mean square error of the regressions is calculated by varying the number of points used in the regression. Figure 14 shows the mean square error versus the number of simulation layers. The optimal number of layers is the one with the minimal mean square error. In the pure statistical case, it is 26 layers. However, this violates the geologic markers by merging different sands, which can significantly impact the flow response as we will see later. This violation underscores the fact the optimal number of layers should be selected based on a combination of geologic insight and statistics rather than purely based on the statistical criterion.

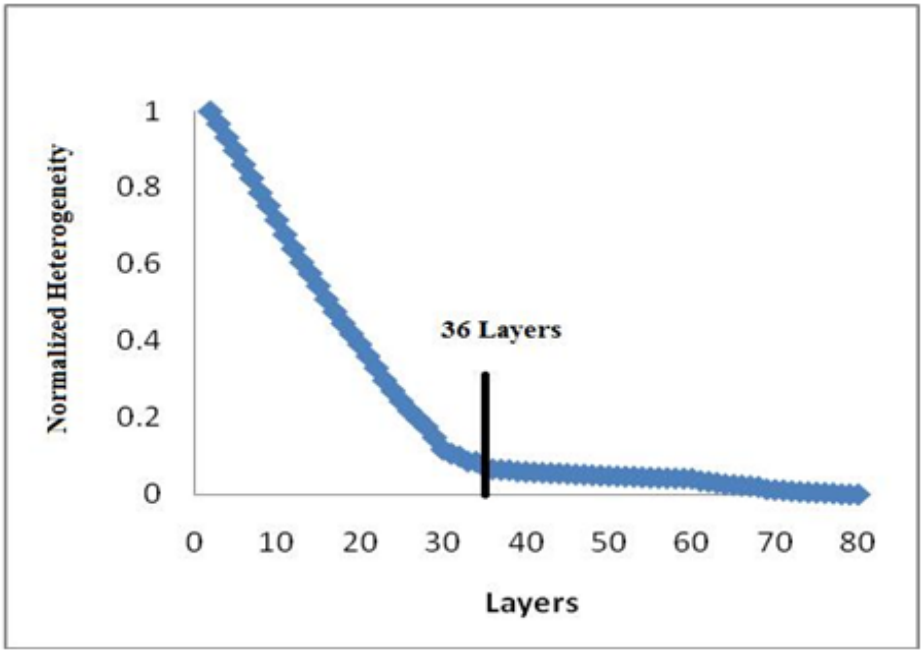

Figure 12 - Normalized heterogeneity analysis.

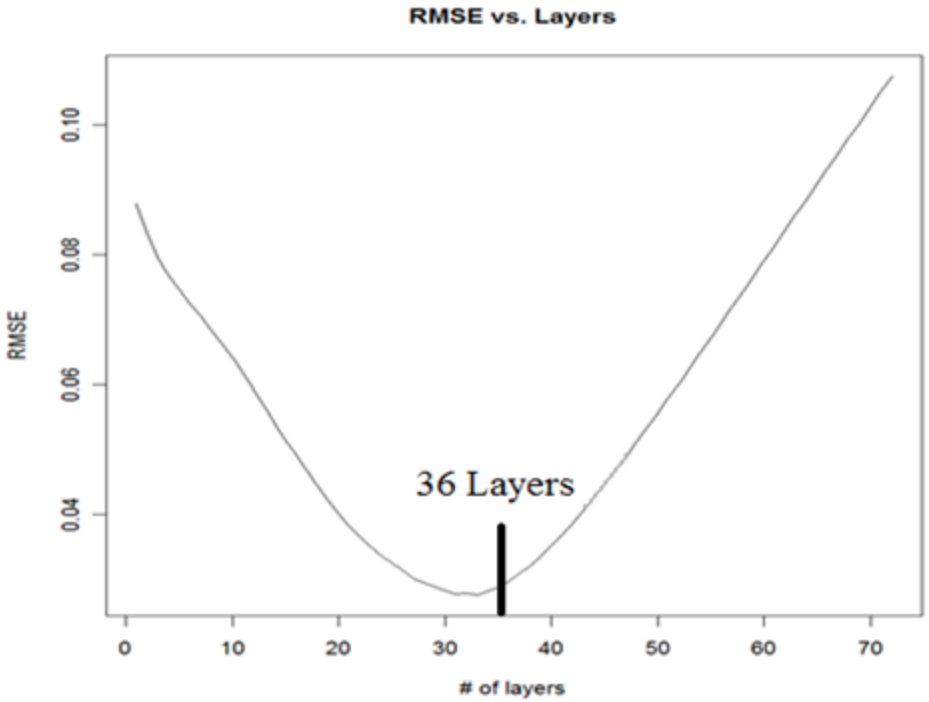

Figure 13 – Layer based statistical regression mean square analysis.

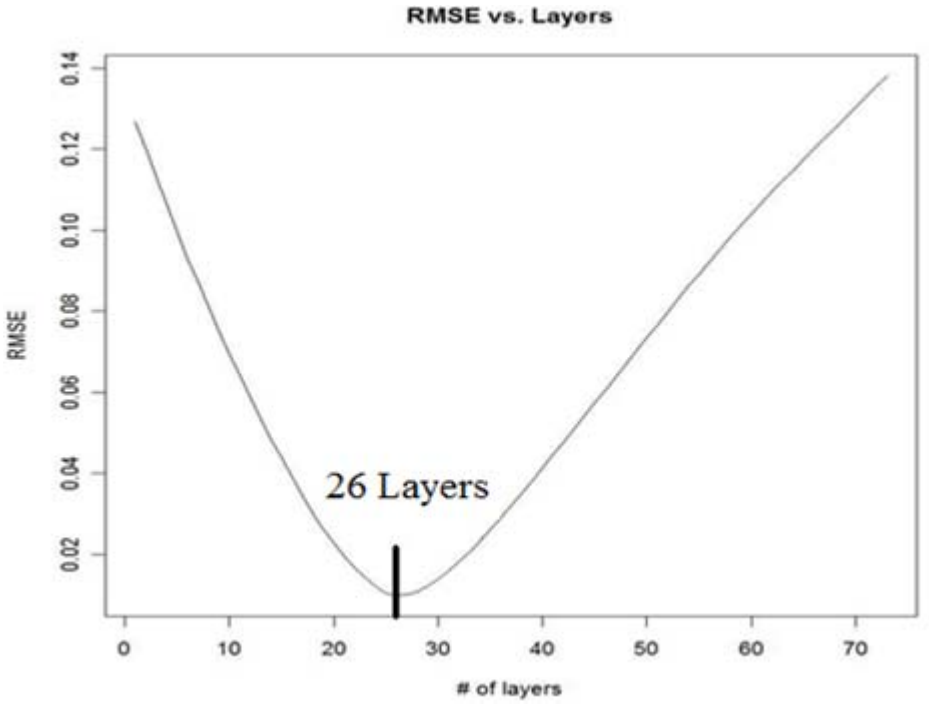

Figure 14 – Pure statistical regression mean square error analysis.

4.3 36 Layer Based Statistical Optimal Model

Figure 15 shows the 3D perspective view of the 36 layer model. Comparing this 3D view with the original 81 layer model as seen in figure 8 it is evident that the model has maintained the same channel characteristics. The 36 layer model has maintained the location and orientation of the channels as in the original earth model with minimal smearing. As expected the range of property values have been altered because of averaging. As mentioned before, the optimal number of layers was determined to be 36 layers because this preserves the distinction between Sand A and Sand B. Sand A as seen in figure 16 shows a decrease in the permeability values when compared to the 81 layer model. However, the main regions of high permeability have maintained their distinction within the layer. The same conclusion can be drawn for Sand B, shown in figure 17**,** as the high permeability regions are maintained on the whole. The main sand is not altered by the upgridding algorithm and this region with distinct resolution of channels is preserved as in the fine-scale model. The field response is compared to the coarse scale model for validation of our algorithm. The 36 layer field response of oil production and water-cut, as shown in figure 18 through figure 20, match excellently with minimal deviation from the fine scale model response. We have included the field response for the 26 layer model in the plots to show the deviation caused by upgridding based upon statistics alone. As a final field scale comparison we compare the field pressure for both the fine scale and coarse model. Figure 21, the field pressure comparison, shows that our upgridded model is an excellent match with the fine scale field pressure. We have also included individual well responses for water cut, oil

production, and bottomhole pressure for a selected number of producers. Figure 22 through figure 27 show the oil production rate, water cut, and bottomhole pressure comparisons for three wells in our model. These wells were chosen as a representative sample of all producers with significant separation between well locations. Production from all three sands is captured in the analysis of these wells. These plots show that our algorithm maintains individual well response excellently as well as the field wide response. The deviation in the bottomhole pressures can be attributed to the well constraints used in our simulation.

The reservoir simulation model constraints are shown in Table 1. The deviation in the bottomhole pressure is caused by the well lowering the pressure to maintain the primary constraint of production rate. As long as the secondary constraint of bottomhole pressure is not violated the well continues to produce. As seen in figure 23 the well in the forecasting period requires a lower bottomhole pressure to maintain the production rate required. This can be attributed to the individual well and its perforation interval which is only in the Sand A. As we saw in figure 16 the Sand A permeability was lowered requiring the bottomhole pressure to be lower than the fine model to produce at the same rate. Typically after a upgridding we expect an improvement in reservoir properties which would require the bottomhole pressure to be higher or equal to the initial model. This is seen in figure 25 and figure 27, where the bottomhole pressure is matching the coarse model and the bottomhole pressure is slightly higher than the coarse model respectively in the forecasting period.

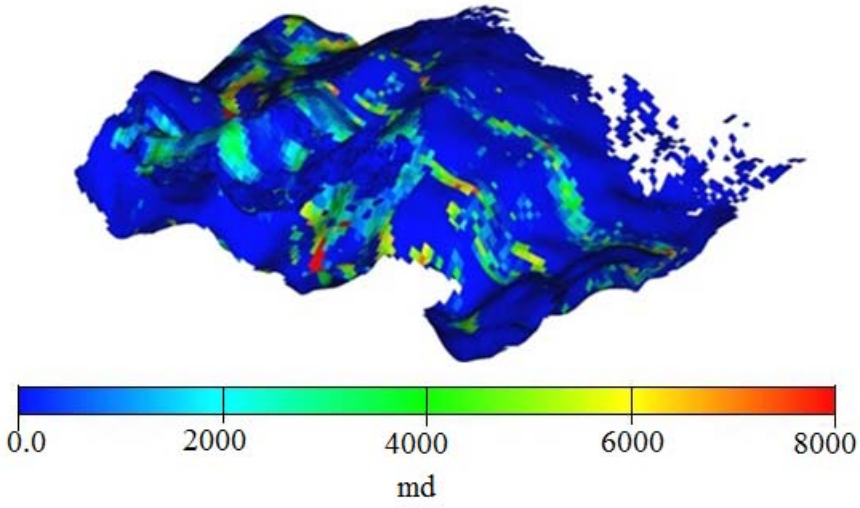

Figure 15 - 36 layer, 3D model permeability distribution.

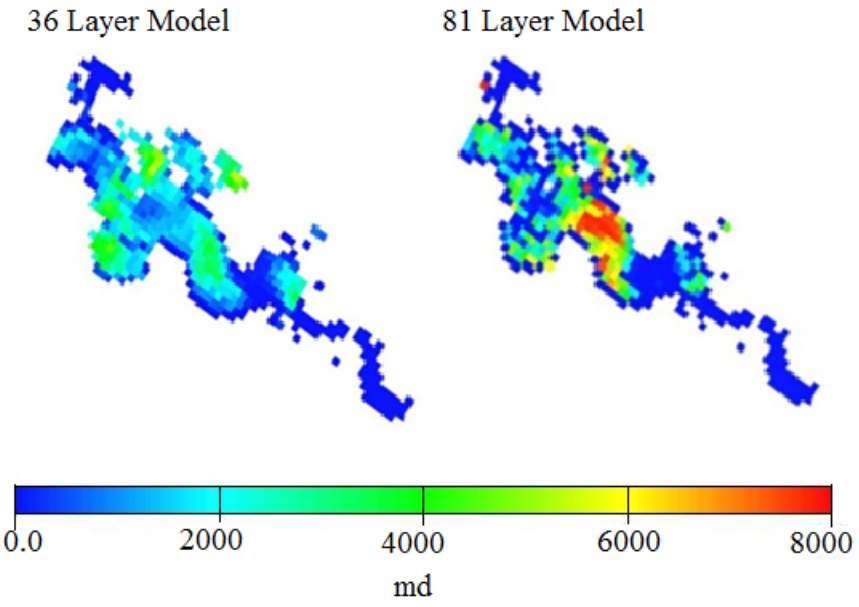

Figure 16 - 36 layer model, Sand A comparison of permeability distribution.

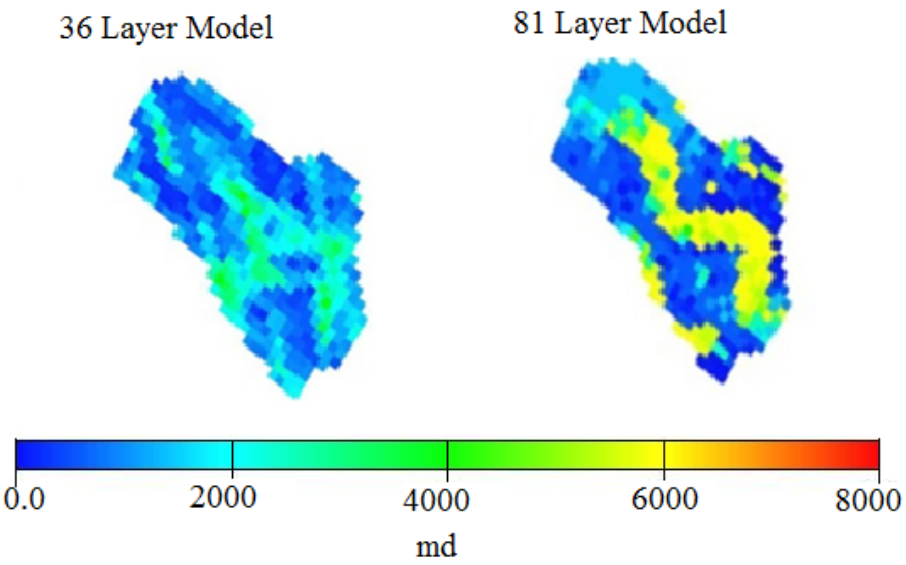

Figure 17 - 36 layer model, Sand B permeability distribution.

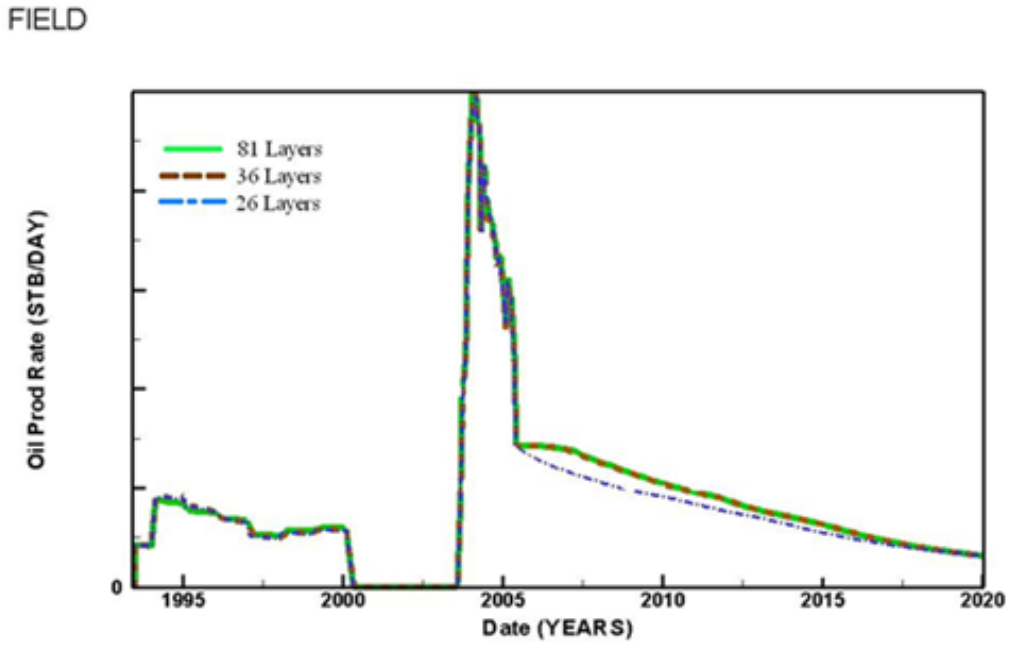

Figure 18 - Field OPR comparison between 36 layers and original model.

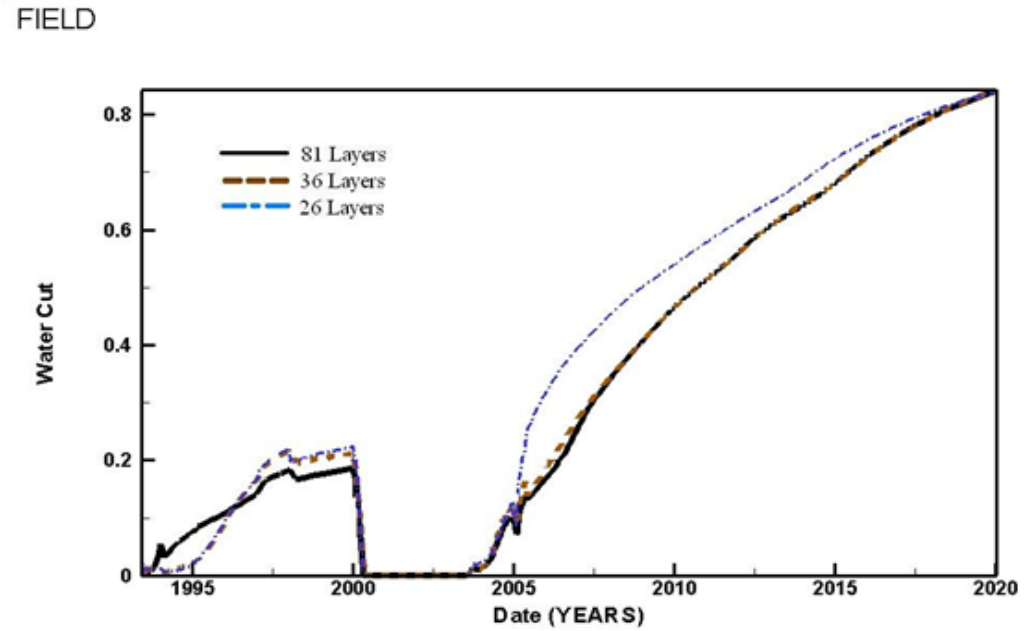

Figure 19 - Field WCUT comparison between 36 layers and original model.

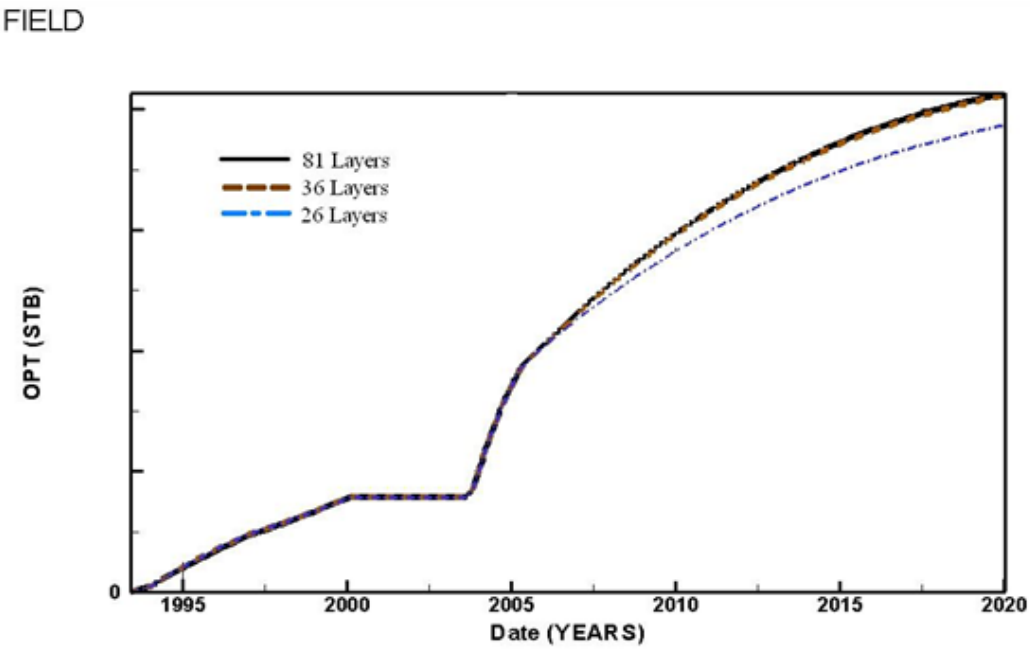

Figure 20 - Field total OPR comparison between 36 layers and original model.

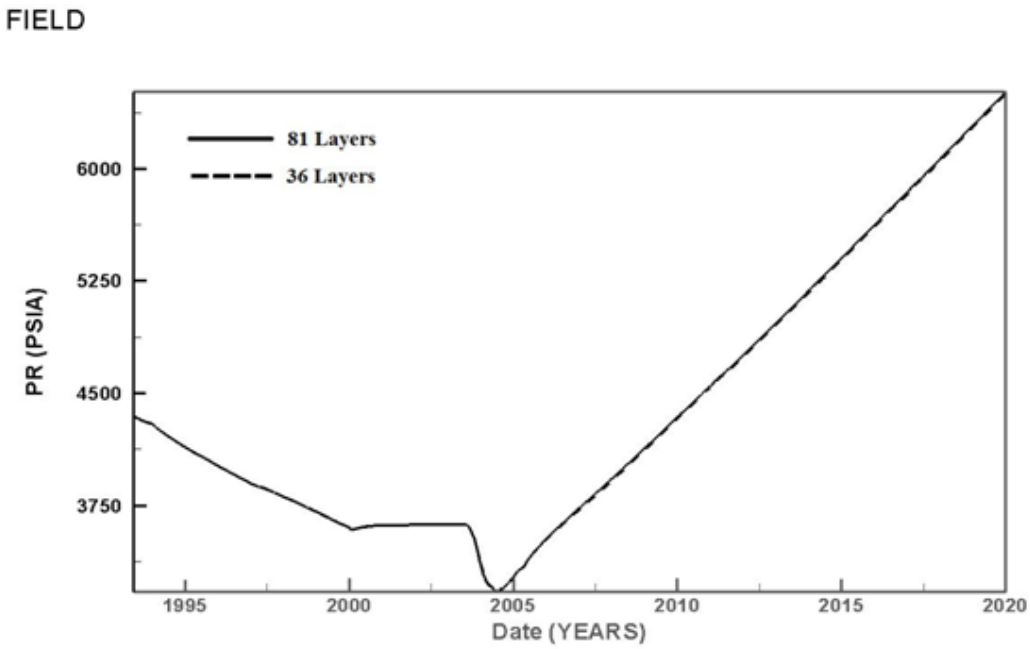

Figure 21 – The field pressure for both the coarse and fine model match.

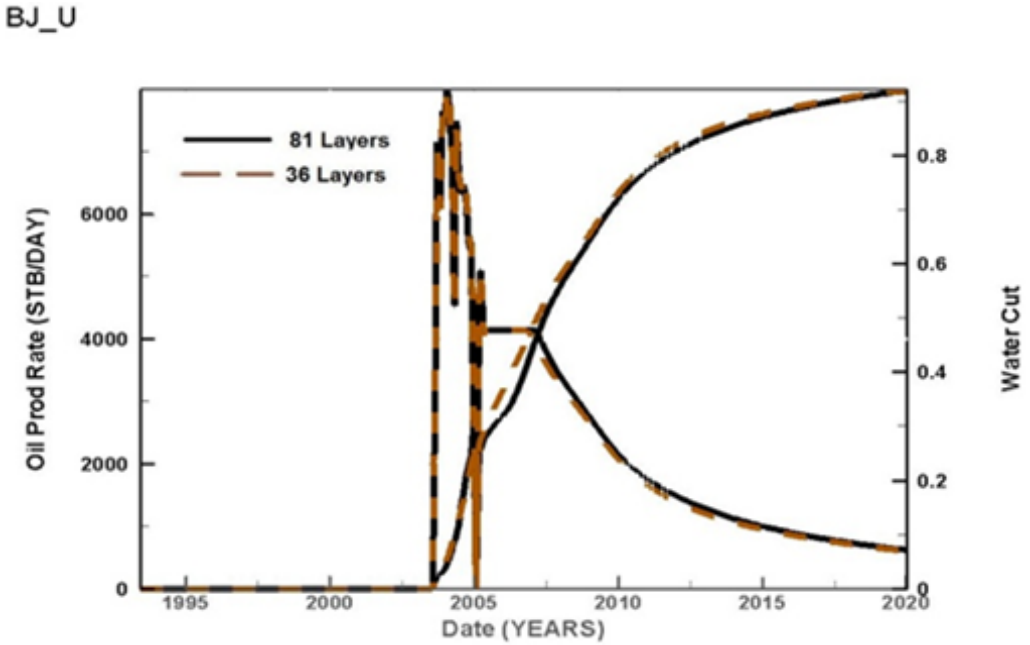

Figure 22 – 36 layer, single well, BJ_U, OPR and WCUT comparison.

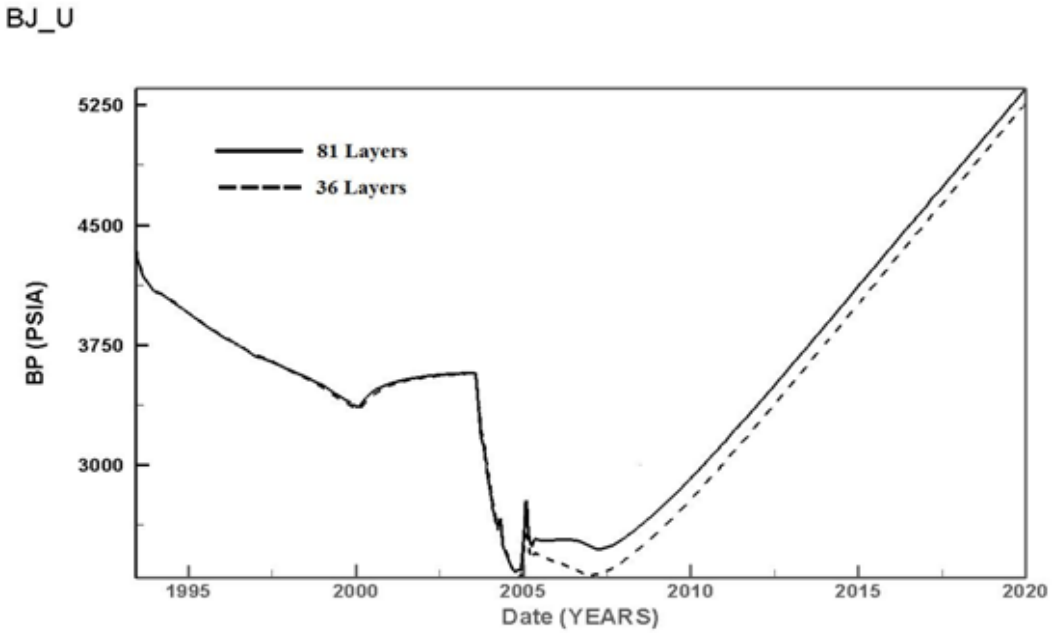

Figure 23 – 36 layer, single well, BJ_U, BHP comparison to the fine scale model.

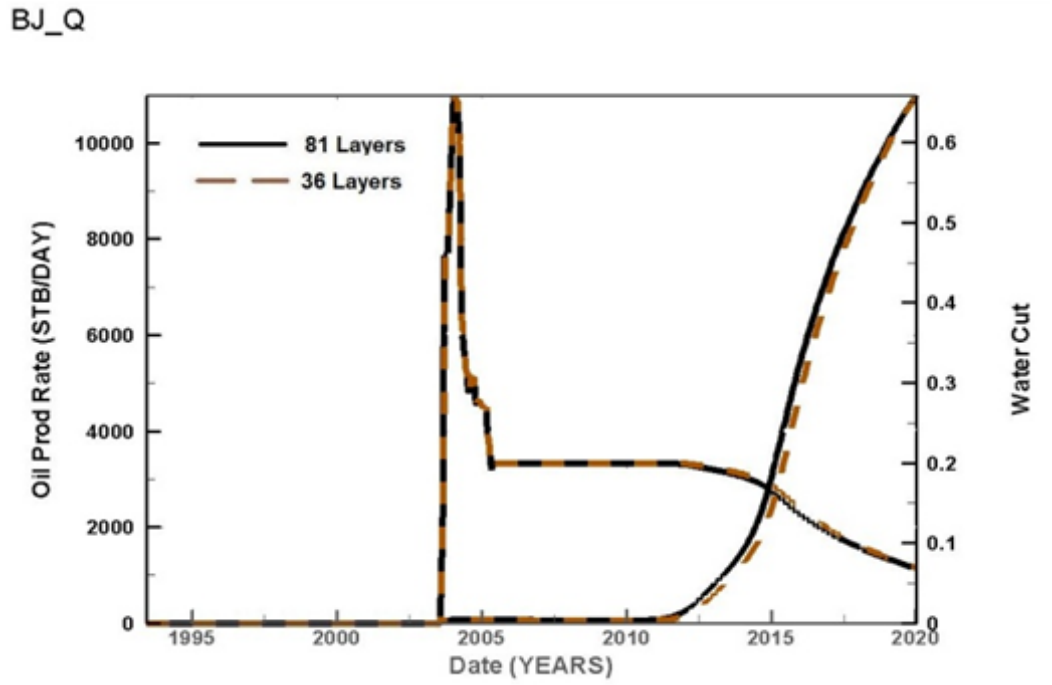

Figure 24 – 36 layer, single well, BJ_Q, OPR and WCUT comparison.

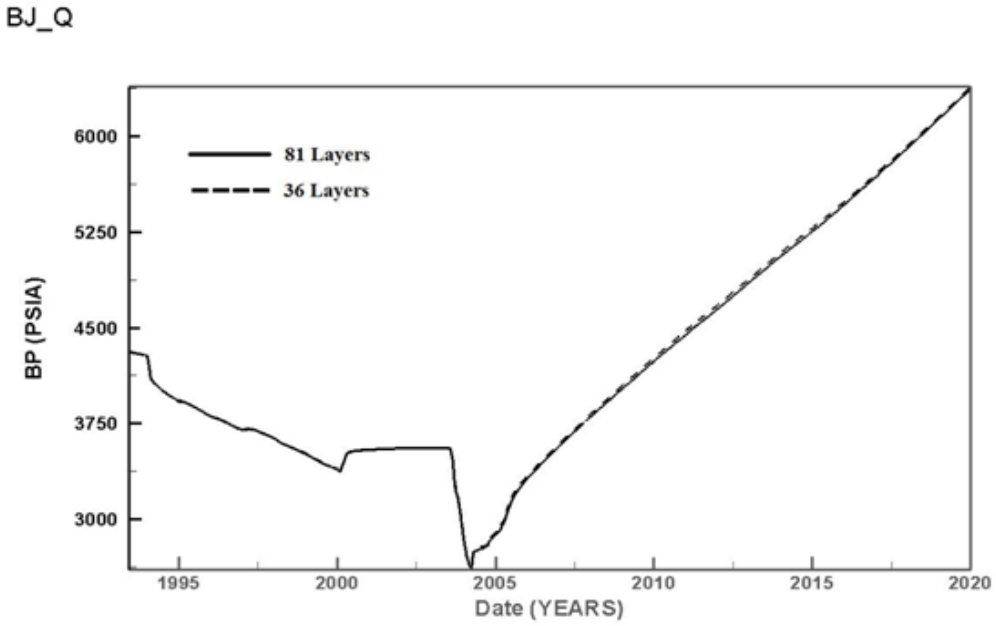

Figure 25 – 36 layer, single well, BJ_Q, BHP comparison to the fine scale model.

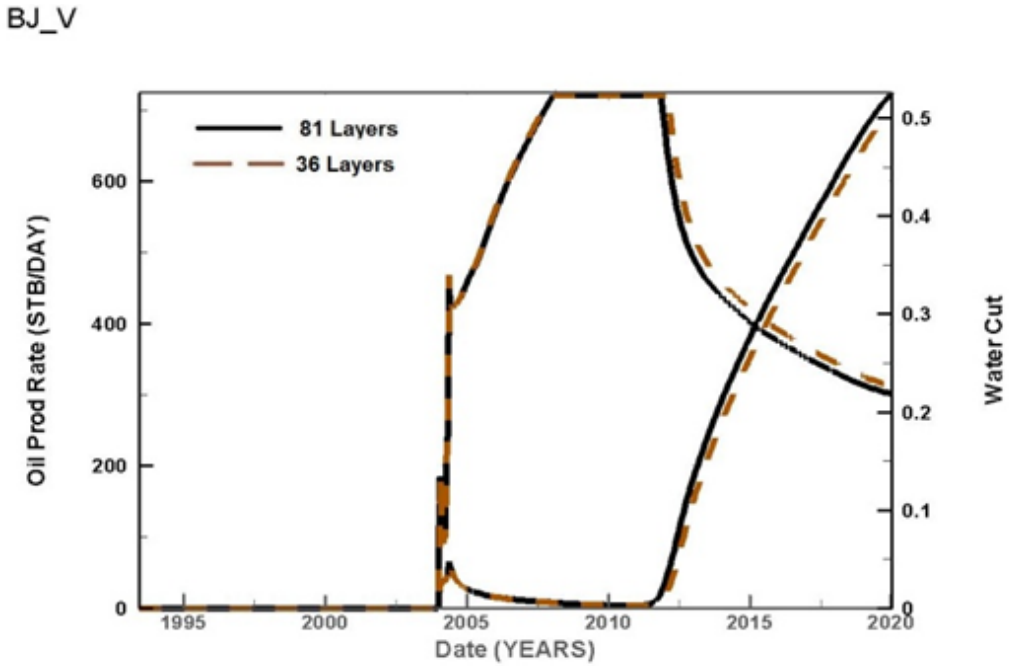

Figure 26 – 36 layer, single well, BJ_V, OPR and WCUT comparison.

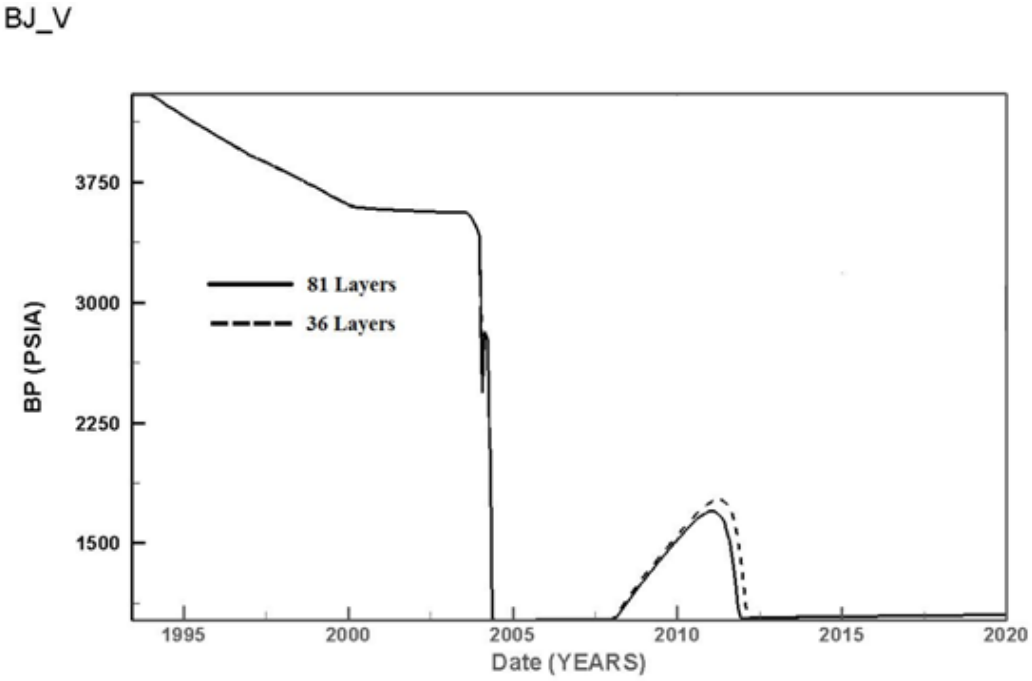

Figure 27 – 36 layer, single well, BJ_V, BHP comparison to the fine scale model.

4.4 Saturation Comparison

Slices of the reservoir in the vertical direction are used to show the water saturation distribution of the fine and coarse scale models. The saturation distribution is an important parameter to validate our optimal upgridding method.

The algorithm we have created recreates the reservoir property files which are then used in a simulation to compare to the fine scale model. The important distinction about our method is that currently the algorithm recreates the property files on the original grid scale. For example if a fine scale model is to be merged from layers 30 to layer 50 our algorithm will reassign the porosity and permeability in layers 30 to layer 50 to a single value in the vertical direction in the layers to be merged. This creates a new coarse model that is technically the fine scale size but simulates as a coarse model. The

saturation therefore is an important parameter to investigate as the simulator assigns saturations during initialization and through production the saturation profiles should closely match for both fine scale and coarse scale models for our algorithm to be considered acceptable.

In the saturation comparison we have investigated both Sands A and Sand B. The Main Sand was not merged in the 36 layer model so the water saturation distribution will be exact matches for both the fine and coarse scale models. Starting with figure 28, which is the first layer of Sand A, we see a slightly higher oil saturation zone as compared to the coarse model. The same conclusion can be drawn for figure 29 which is the same layer after 7 more years of production. The saturation distribution pattern is similar to the coarse models with the only minor differences in the saturations. This saturation difference can be attributed to the fact that upgridding will improve the reservoir properties in previously underperforming layers and therefore enhance the reservoir performance. The improved flow performance requires less production from each layer to maintain the required production. This creates higher oil saturations in the upgridded layers. Figure 30 and figure 31, both of which are the 16^{th} layer of Sand A, show the same trend as seen in the first layer of Sand A. The same conclusions are drawn for Sand B, which is profiled in figure 32 and figure 33, as the same saturation distribution pattern is seen with minor differences occurring in the saturation levels.

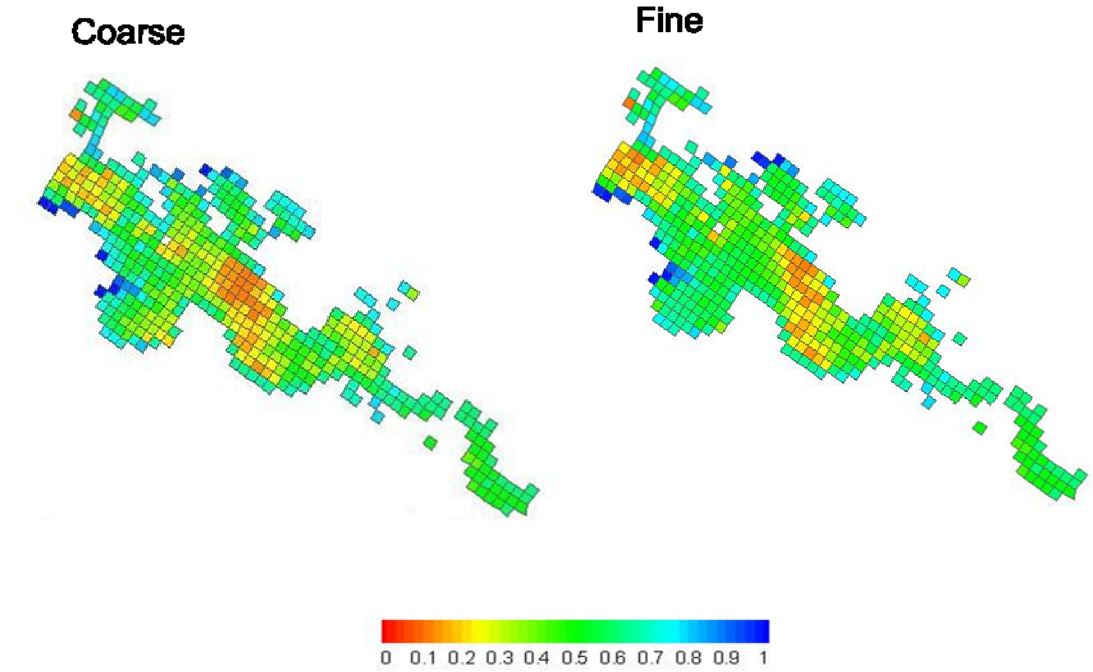

Figure 28 – Sand A, layer 1, water saturation comparison at production year 2013.

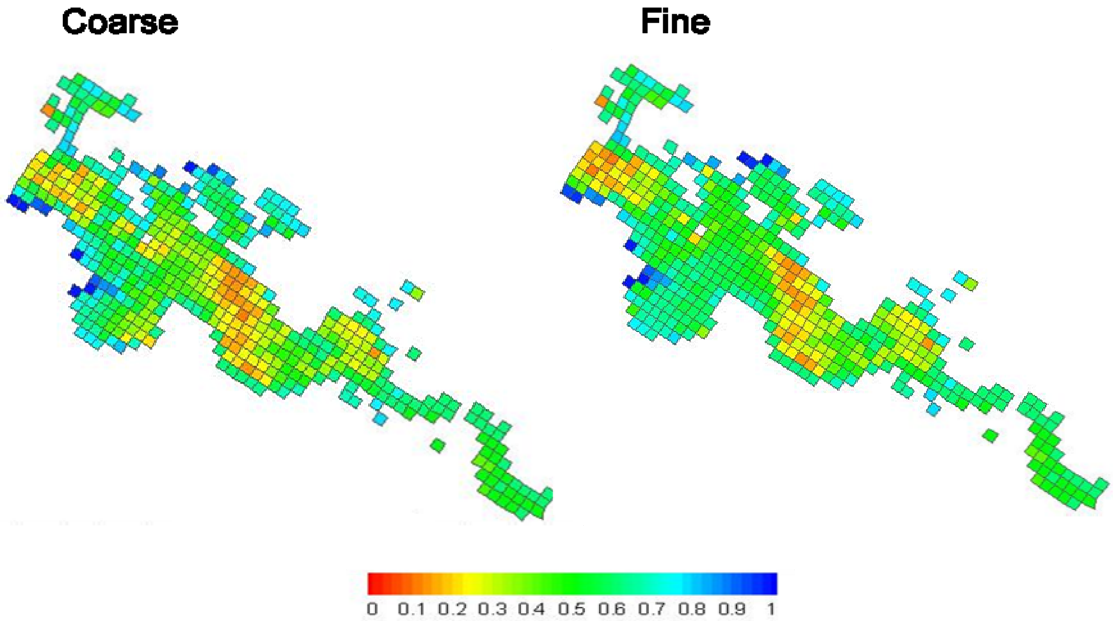

Figure 29 – Sand A, layer 1, water saturation comparison at production year 2020.

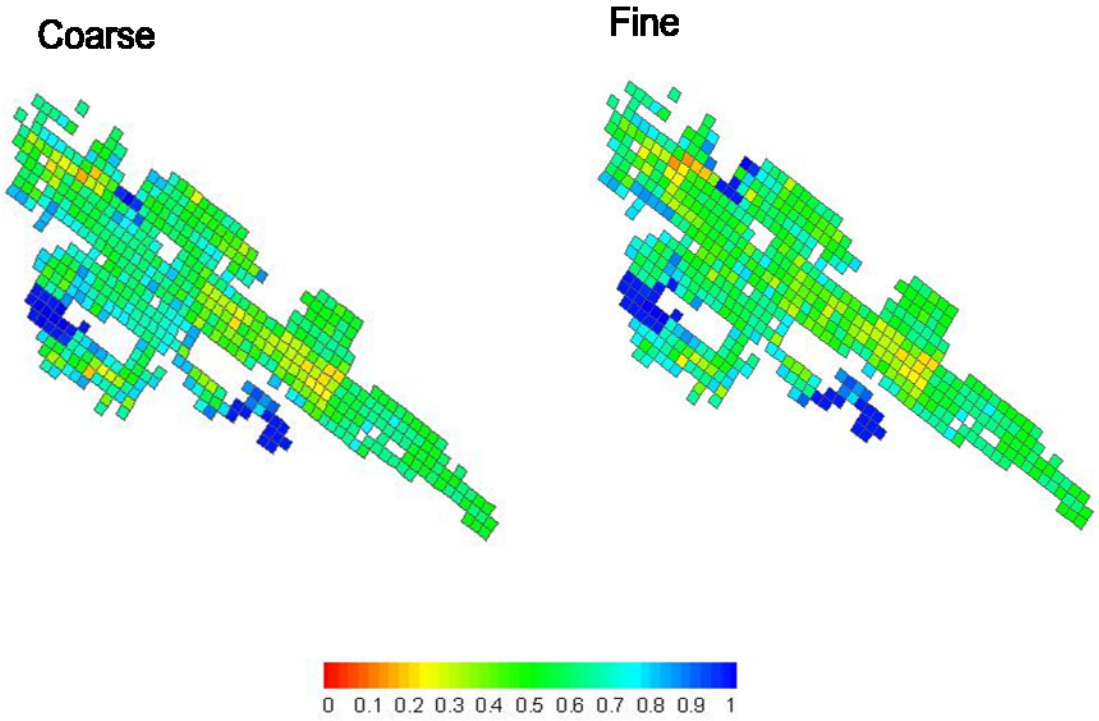

Figure 30 – Sand A, layer 16, water saturation comparison at production year 2013.

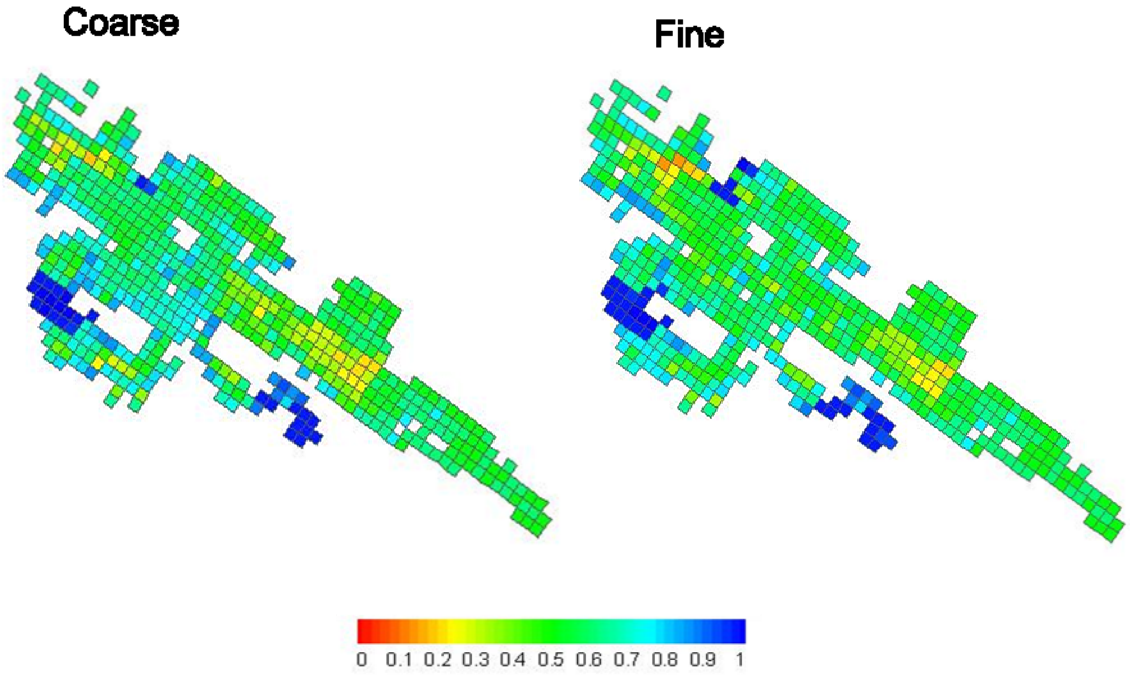

Figure 31– Sand A, layer 16, water saturation comparison at production year 2020.

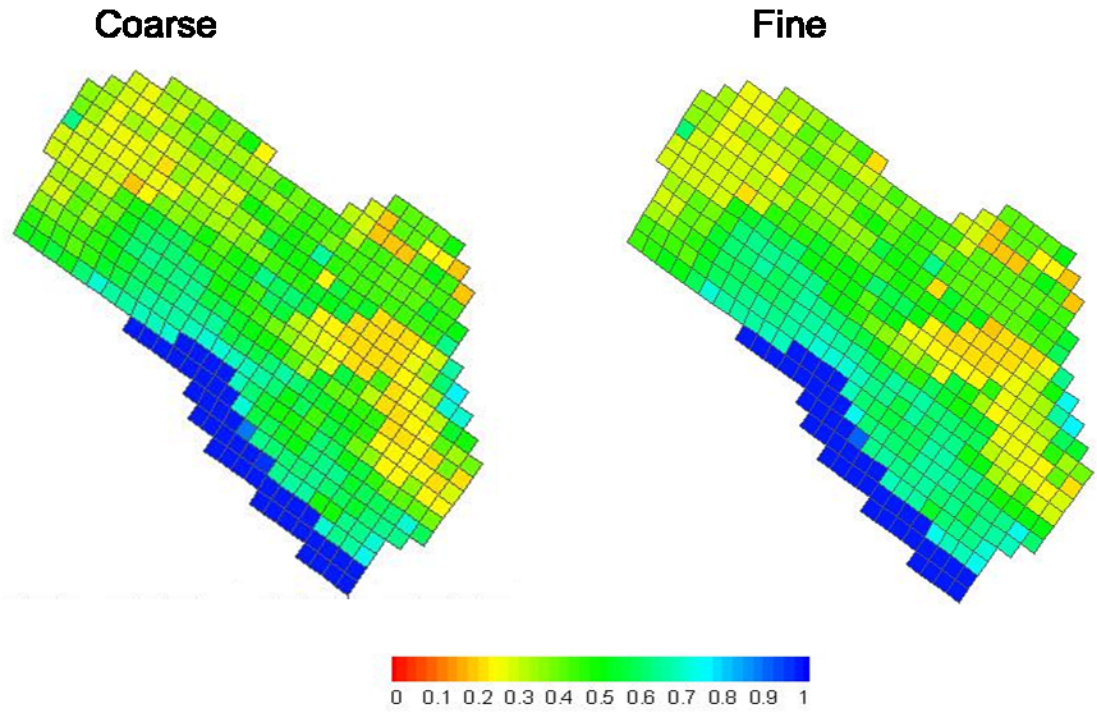

Figure 32 – Sand B, layer 34, water saturation comparison at production year 2010.

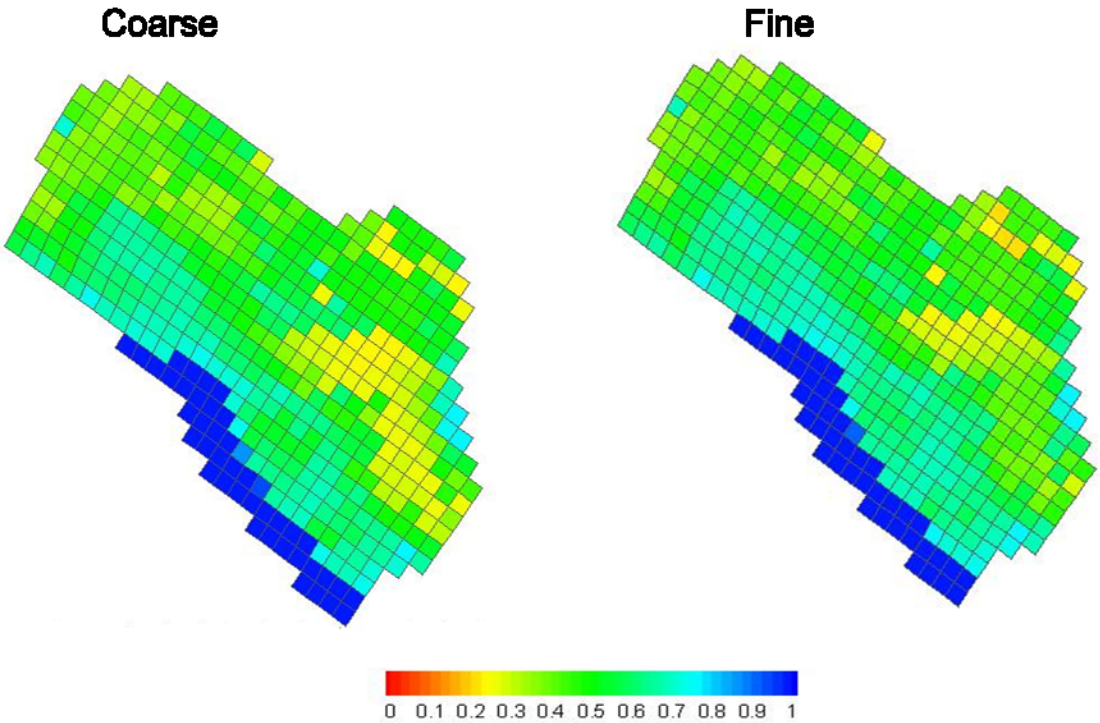

Figure 33 – Sand B, layer 34, water saturation comparison at production year 2016.

4.5 26 Layer Pure Statistical Optimal Model

As mentioned before, an analysis of the ‘within the cell variation (W)’ curve without regard to the geologic markers will lead to 26 layers as being optimal. The 3D model with 26 layers as seen in figure 34 shows that the reservoir properties have been significantly smeared compared to the original distribution as channels have been removed from the model. The choice of 26 layers results in the loss of the facies distinction between all sands from layer 1 to layer 56. This merges all of Sands A and Sand B and the top 4 layers of the Main Sand. The reservoir response is also altered because the reservoir properties are smeared and lowered below their appropriate values as layers are merged across geologic boundaries. Figure 35, Sand A, and figure 36, Sand B, show the merging of these sand bodies causing a severe lowering of the reservoir properties and loss of channels. The Main Sand, shown in figure 37, compares the permeability of the 81 layer and 26 layer models. This comparison shows a major loss of geologic resolution when merging across sand body markers. Figure 38 through figure 40 show the reservoir response of the fine scale model compared to the 26 layer model on an individual well response. The same individual wells are used for comparison as were used in the 36 layer model. It is evident that the reservoir properties are altered significantly causing a significant deviation in water cut and therefore a deviation in oil production rate as seen in all the individual well plots. The field wide response as expected from the individual well analysis is significantly deviated from the fine scale model as seen previously in figure 18 through figure 20.

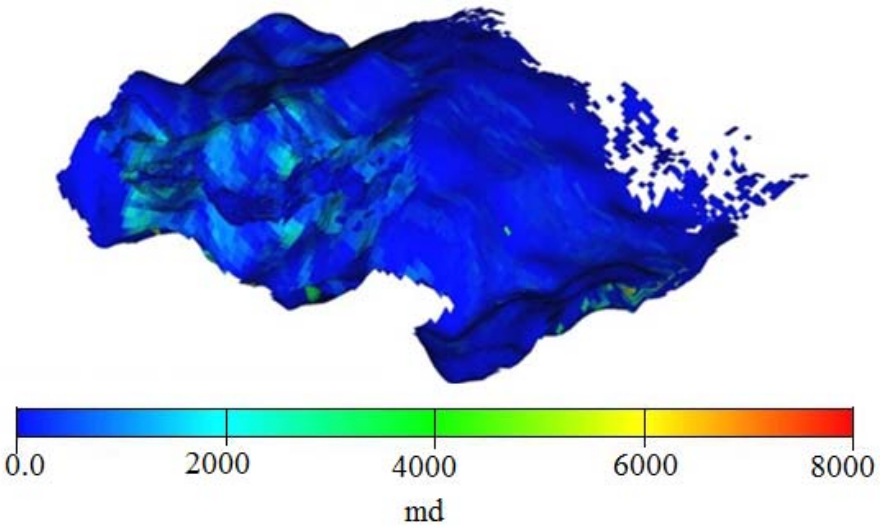

Figure 34 - 26 layer, 3D model permeability distribution.

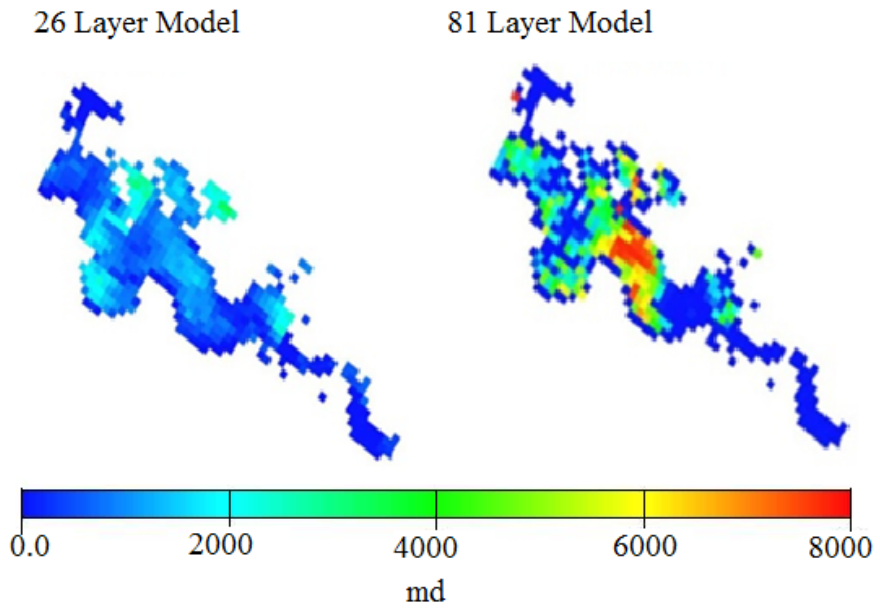

Figure 35 - 26 layer model, Sand A permeability distribution comparison.

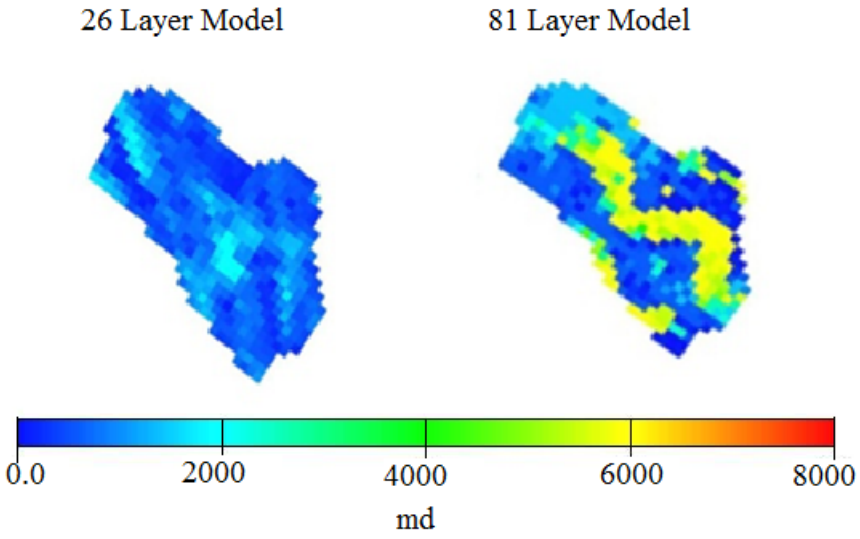

Figure 36 - 26 layer model, Sand B permeability distribution comparison.

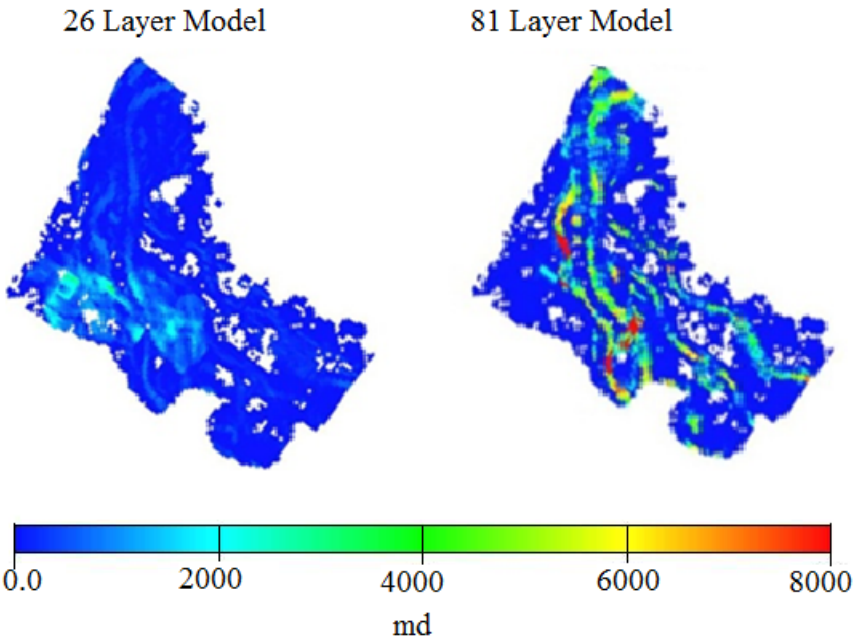

Figure 37 - 26 layer model, Main Sand permeability distribution comparison.

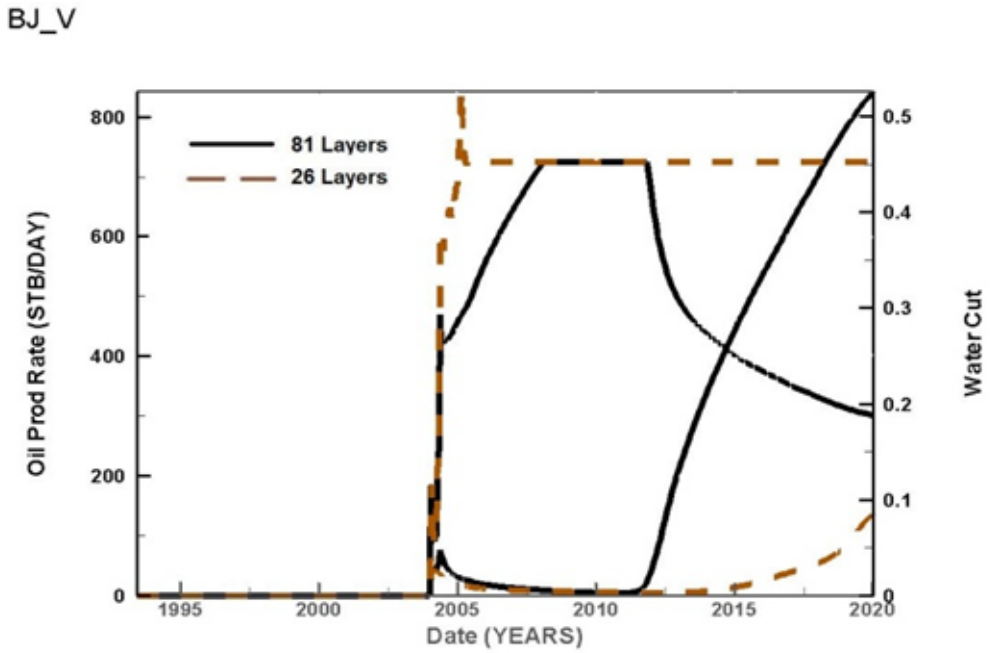

Figure 38 – 26 layer, single well, BJ_V, OPR and WCUT comparison.

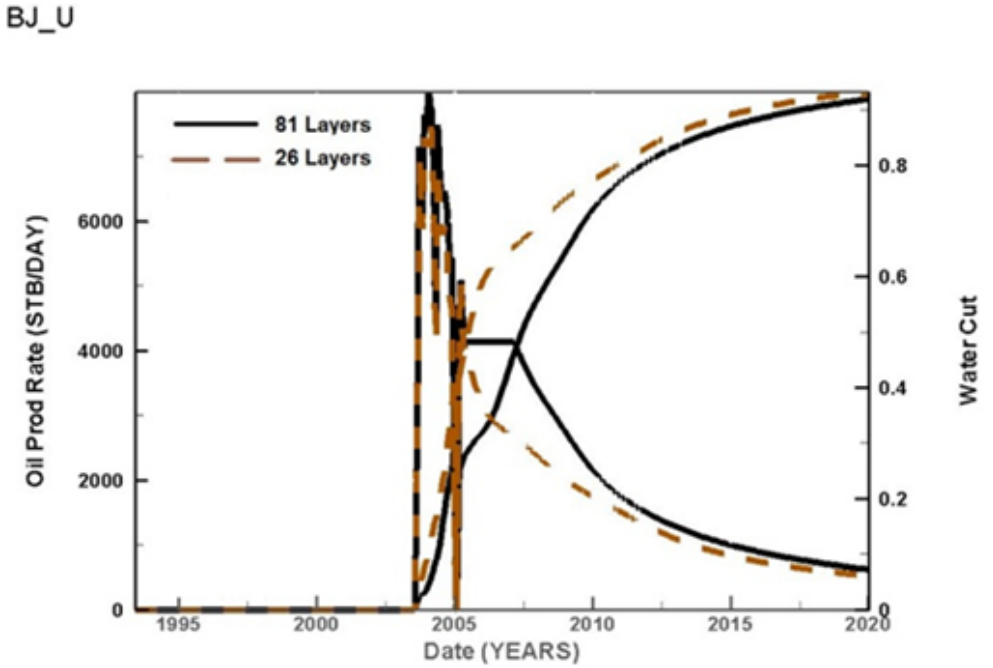

Figure 39 – 26 layer, single well, BJ_U, OPR and WCUT comparison.

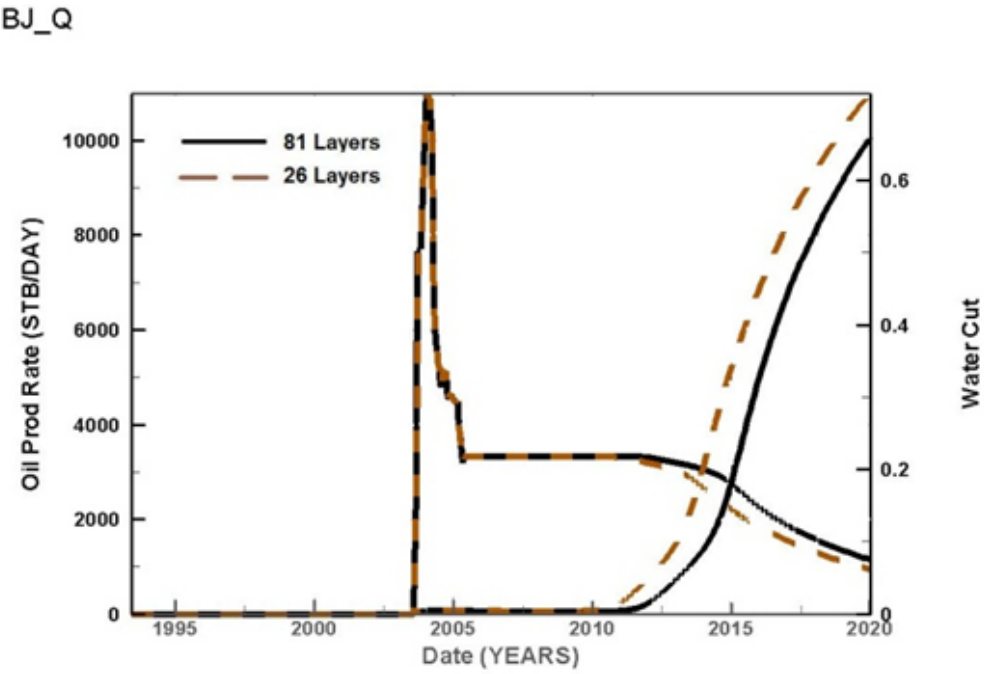

Figure 40 – 26 layer, single well, BJ_Q, OPR and WCUT comparison.

4.6 Uniform Upgridding

We have also compared our results against uniform upgridding to examine the potential benefits from our approach. We wrote another program that will perform uniform upgridding up until the last even number layer. The model simply uses bulk volume weighted averages in the column index for each cell in the layers that are to be merged. The software then outputs the new property files that simulate a uniform upgridding procedure. The original 81 layer model was uniformly upscaled to 41 layers by merging the first 80 layers in sets of two. This leaves layer 81 as an unaltered layer due to the odd number of layers in our fine scale model. The upgridding algorithm alters the reservoir properties to a 41 layer equivalent model but remains on the 81 layer scale. We then reran the flow simulation to compare the reservoir response with our algorithm for

upgridding. The goal here is to compare the smearing of permeability distribution of the channels when using a uniform upgridding approach. The field wide response to uniform upgridding was fairly reasonable with deviation from the fine scale model evident but not as significant as compared to the individual well responses. Figure 41 through figure 43, shows the oil production rate and water-cut for the selected wells. The response is significantly altered from the fine scale model. This is due to the smearing of the reservoir properties and loss of geological realism due to upgridding across sand markers and merging pay/non-pay regions.

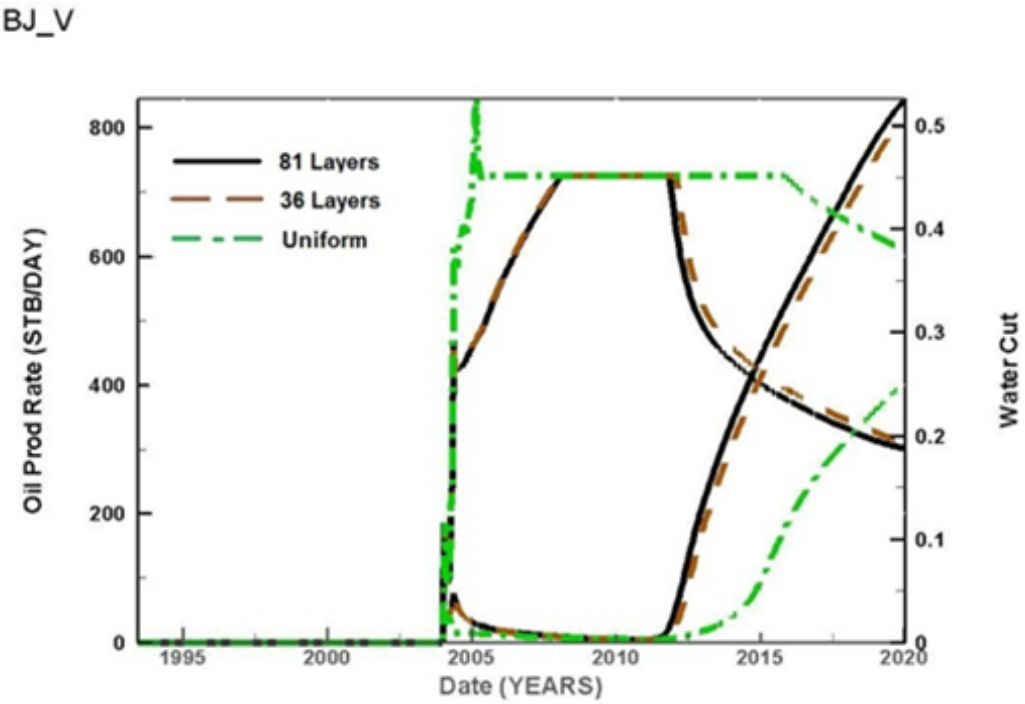

Figure 41 – Uniform upgridding, single well, BJ_V, OPR and WCUT comparison.

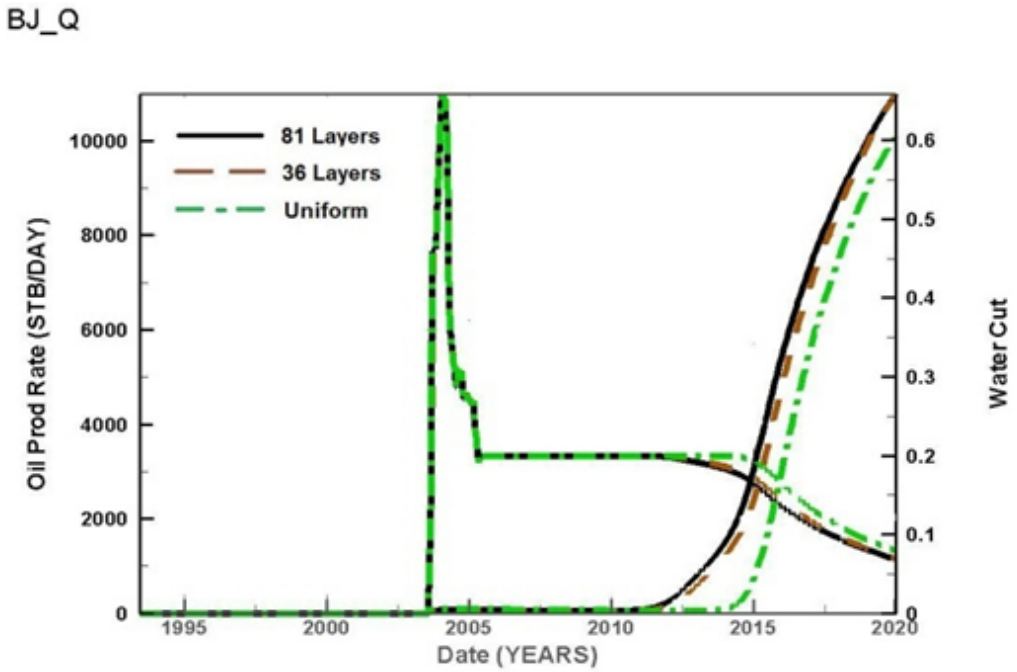

Figure 42 – Uniform upgridding, single well, BJ_Q, OPR and WCUT comparison.

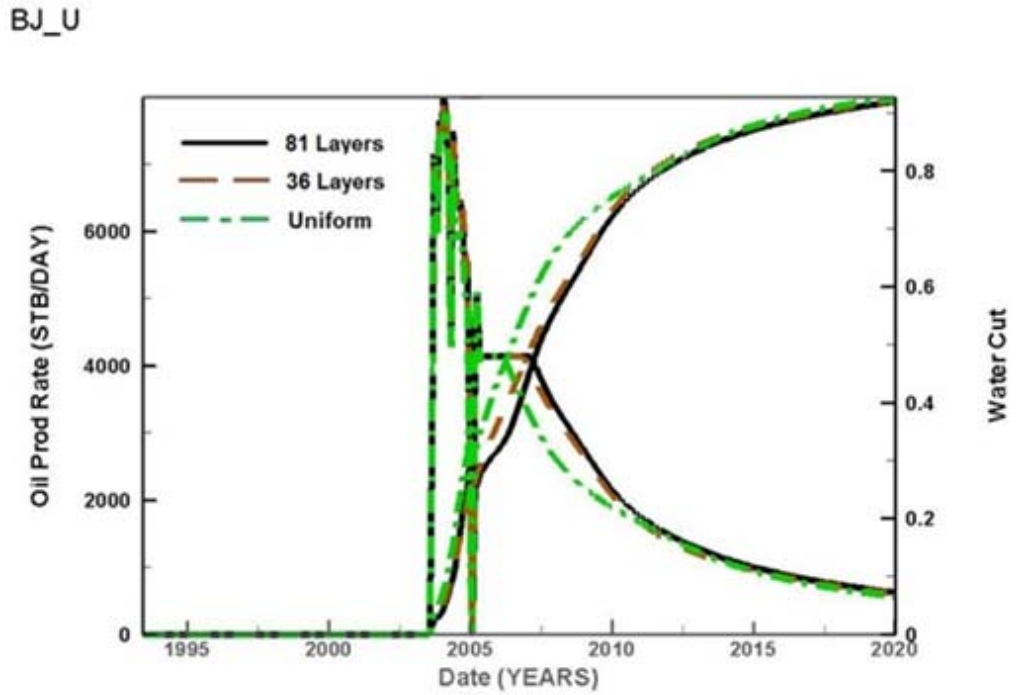

Figure 43 – Uniform upgridding, single well, BJ_U, OPR and WCUT comparison.

5. TIGHT GAS RESERVOIR

The second case study we applied our algorithm to is a proprietary reservoir model to Schlumberger DCS. The location, production history, and well information are not available for publication and therefore our results will be analyzed visually using a section located in the middle of the reservoir.

The field was analyzed with both the pure statistical optimization and the layer based statistical algorithm. Schlumberger's reservoir model was created using 14 separate zones which are outlined in Table 2. The fine scale model porosity is shown in figure 44, the areal distribution, and figure 45, the vertical distribution. Not much information can be obtained from the areal distribution however it is evident in the vertical distribution that the original 1347 layer model has many sharp changes between low and high porosity as characterized by tight gas reservoirs. The same conclusion is drawn when investigating figure 46, the areal distribution of permeability, and figure 47, the vertical permeability distribution.

Table 2 – Zone Information for Tight Gas Sandstone.

Zone	Thickness	Bottom Layer
1	203	203
2	166	369
3	30	399
4	186	585
5	98	683
6	69	752
7	26	778
8	78	856
9	94	950
10	58	1008
11	84	1092
12	34	1126
13	151	1277
14	70	1347

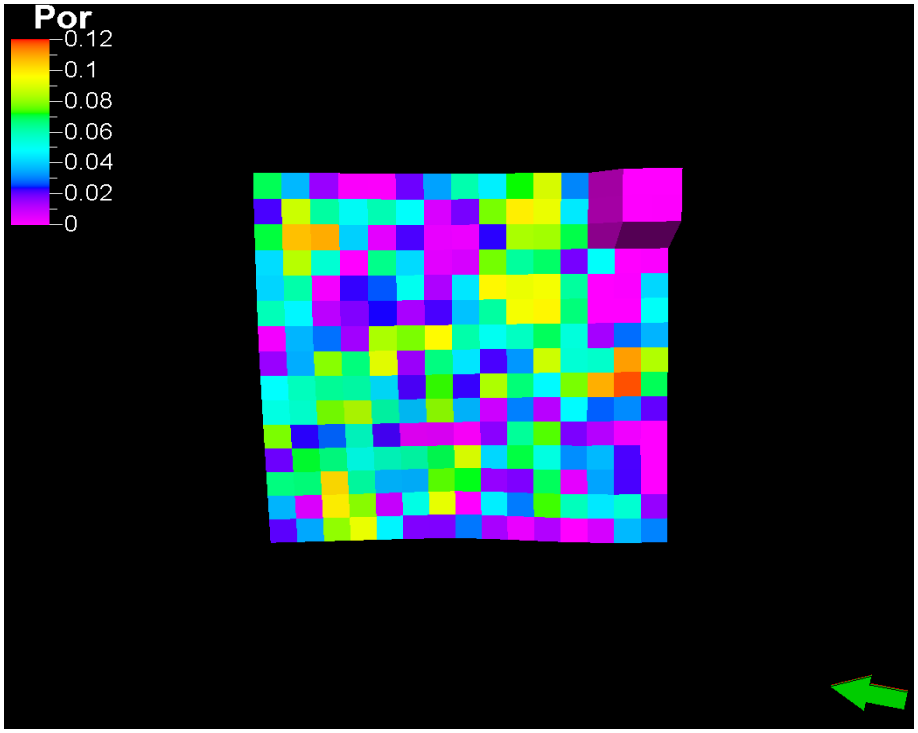

Figure 44 – Areal porosity distribution for fine model.

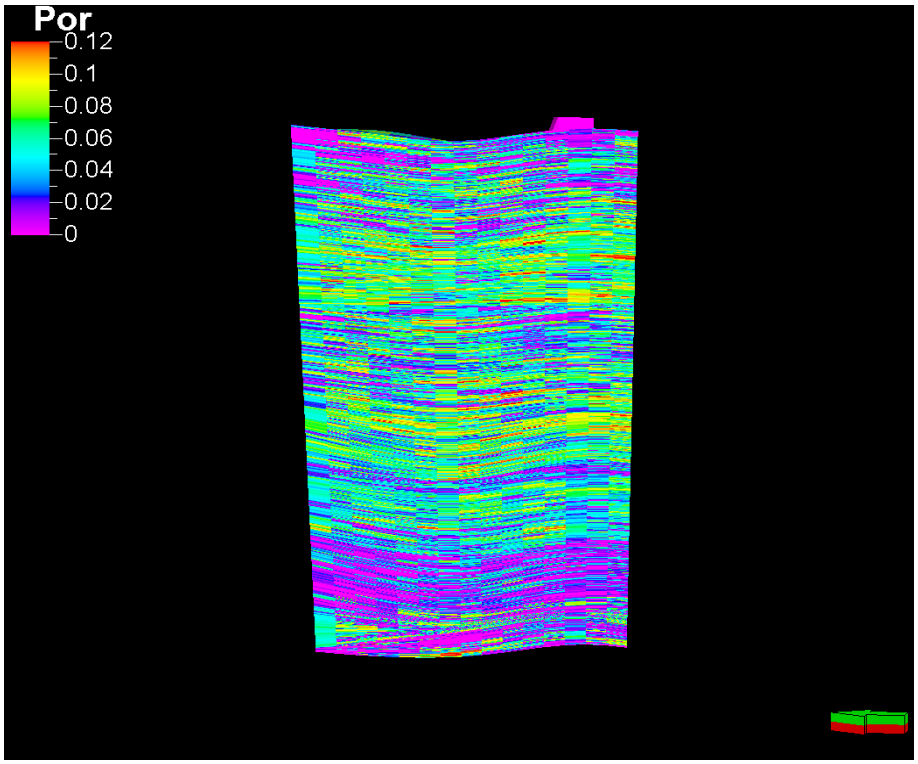

Figure 45 – Vertical porosity distribution for fine model.

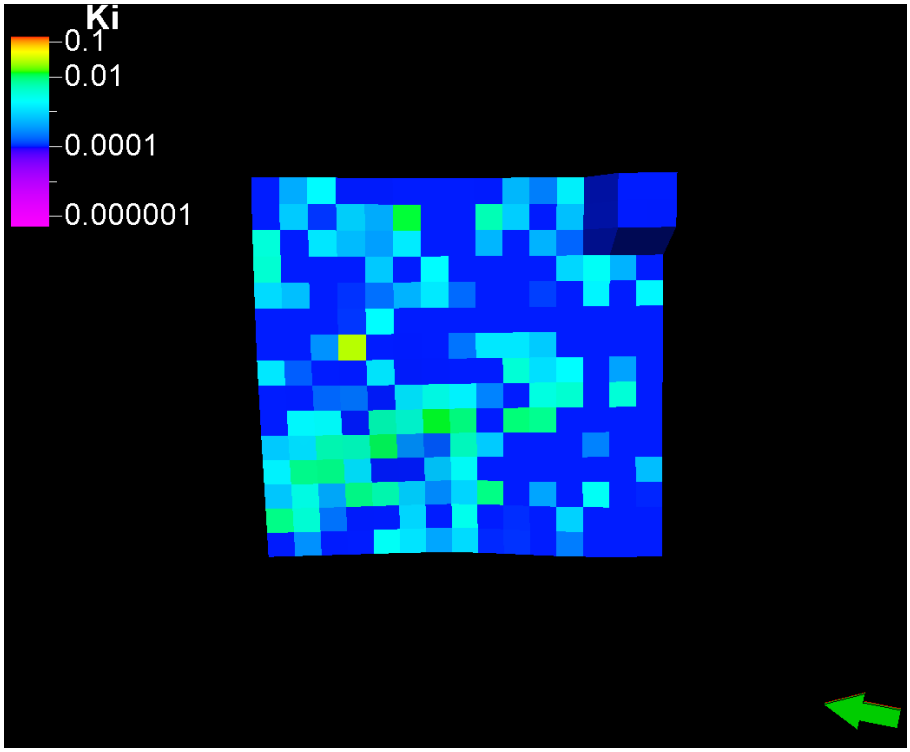

Figure 46 – Areal permeability distribution for fine model.

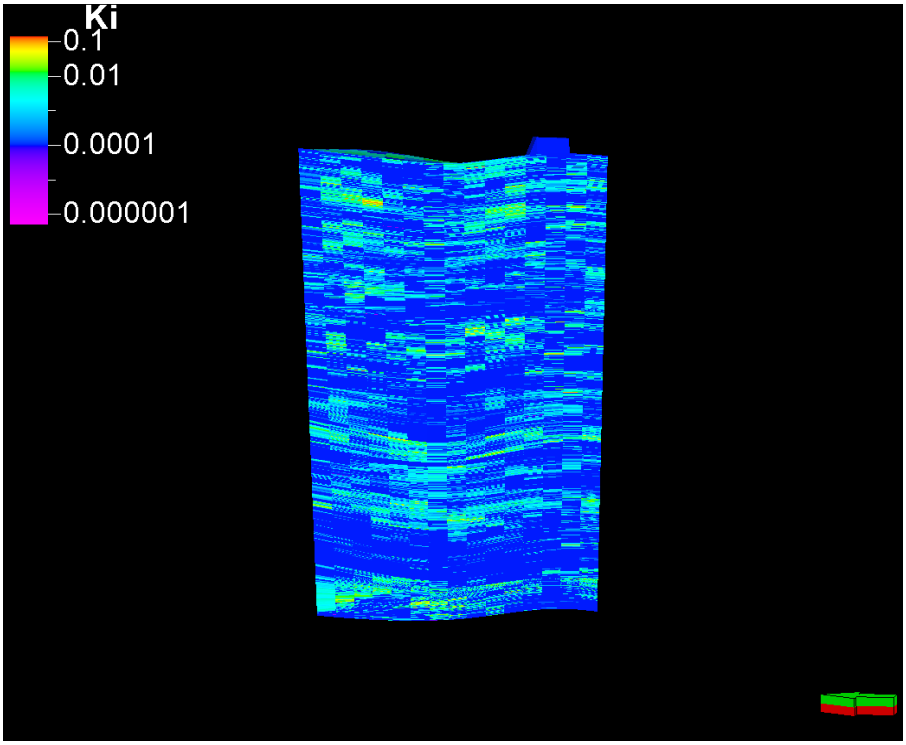

Figure 47 – Vertical permeability distribution for fine model.

Our first analysis uses the pure statistical algorithm. This allows our optimization to merge across the zone boundaries outlined in the bottom layer column of Table 2. Analyzing our within heterogeneity removed vs. layers using the R statistical software we arrive at an optimal model with 229 layers. Figure 48 shows our R analysis plot and determination of the optimal layering. Schlumberger's original model was exported from Petrel as a section with the updated reservoir properties as calculated by our algorithm. The original reservoir model has 2,521,584 cells and it is not possible to simulate. We investigate a section, 15x15x1347, to compare our upgridding algorithm to the fine scale model. The sectioning creates a model that has 303,075 active cells and is easier to visually compare. The porosity distribution of our section is shown in figure 49 through figure 50. It is evident that in figure 49 our porosity distribution varies in the areal direction while figure 50 shows that in the merged zones the properties have been homogenized in the vertical direction according to our merging sequence. We have also provided the permeability distribution plots as shown in figure 51 and figure 52 which show the same trends as previously discussed in the porosity investigation. The pure statistical optimization has merged layers 92 through 903. This has severely violated the zone information by merging zones 1 through 9. These zones were created in the original model because the field has hydraulic fractures which do not breakthrough the zone in which the fracture was placed. This is another example of the requirement that our algorithm maintain the separation between zones if the information is available to the user.

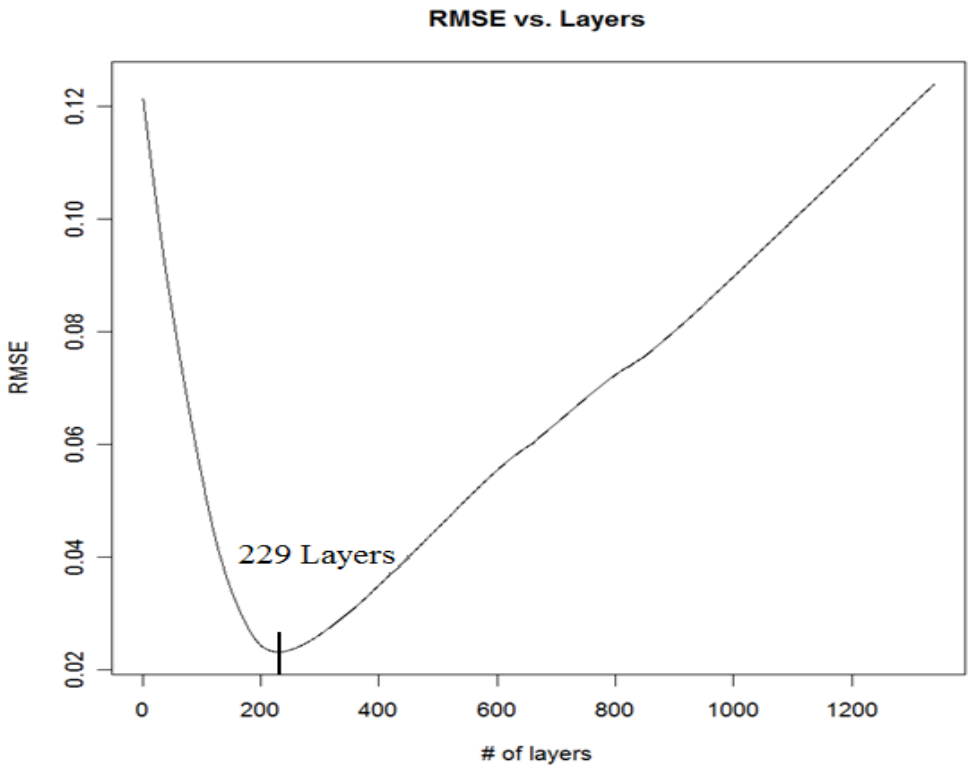

Figure 48 - 229 pure statistical model RSME analysis.

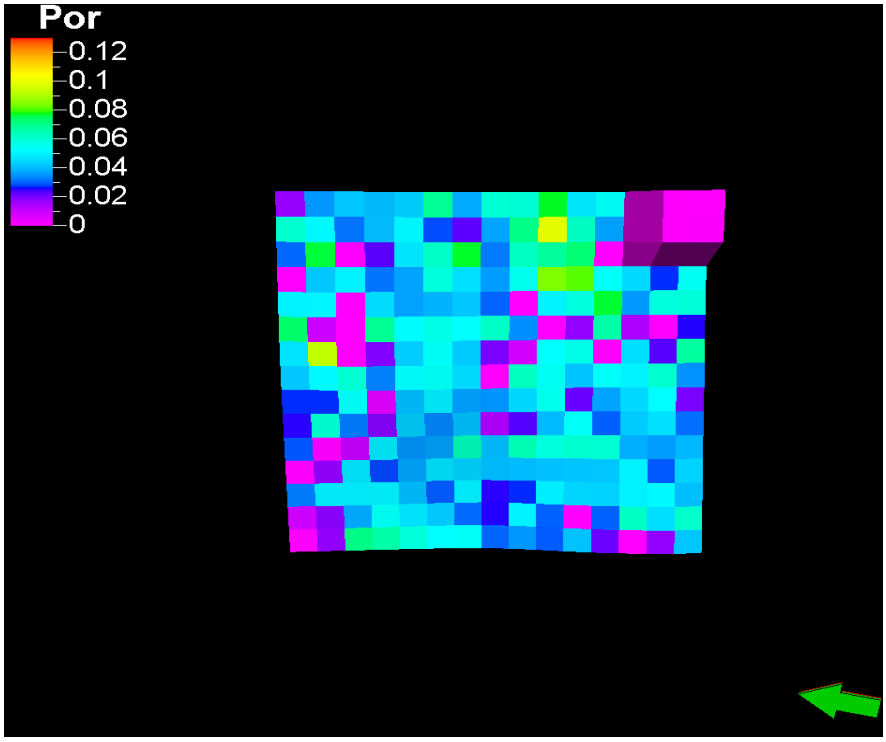

Figure 49 – Areal porosity distribution for 229 layer model.

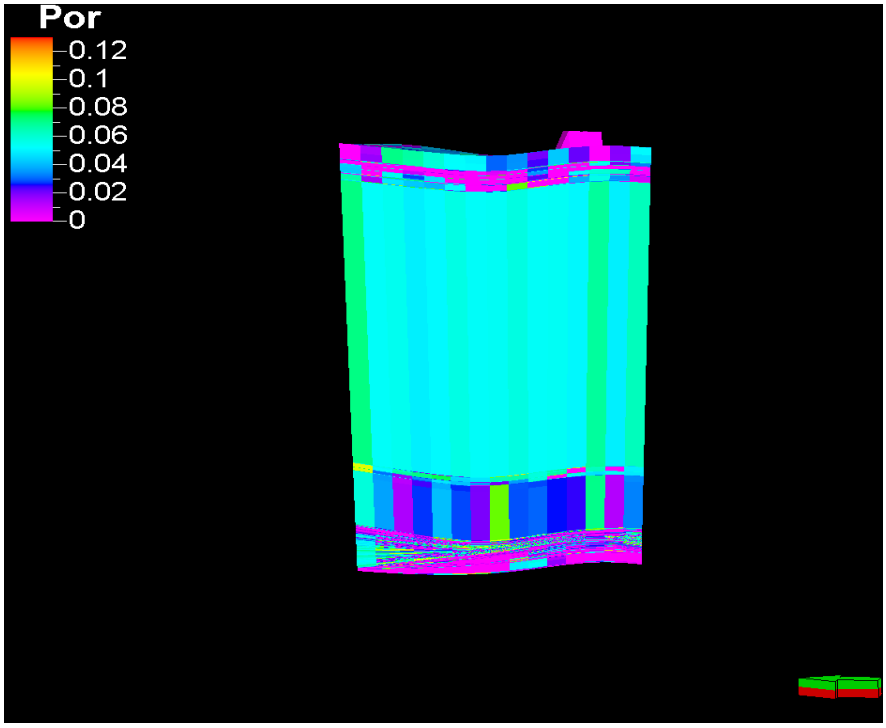

Figure 50 – Vertical porosity distribution for 229 layer model.

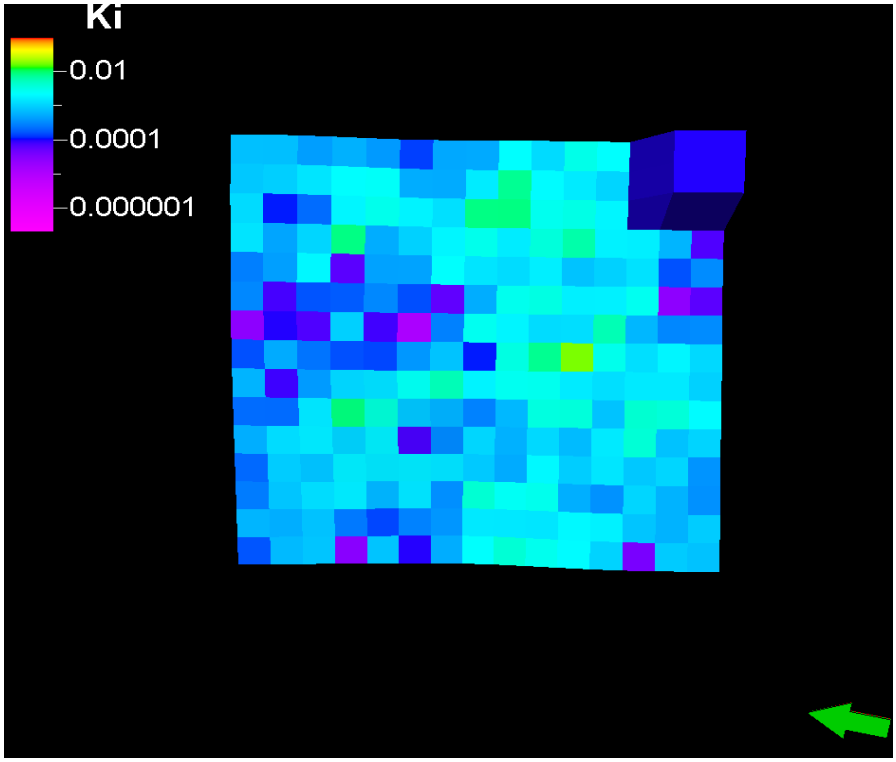

Figure 51 – Areal permeability distribution for 229 layer model.

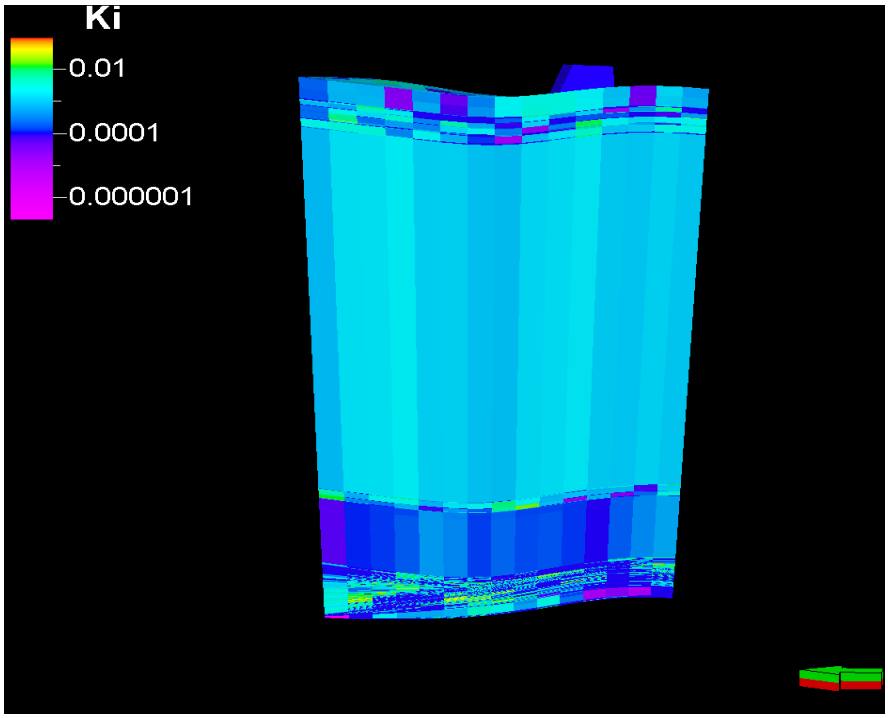

Figure 52 – Vertical permeability distribution for 229 layer model.

Our second analysis uses the layer information to optimally upgrid the reservoir. Applying the R statistical software analysis to our heterogeneity removed information we arrive at the optimal layering of 253 layers as shown in figure 53. This analysis keeps all 14 zones separated and upgridding only occurs in each independent zone resulting in some zones being reduced to 1 layer. Figure 54 through figure 55 shows the areal and vertical distribution of porosity respectively in our layer optimized model. Figure 56 through figure 57 shows the permeability distribution in the areal and vertical direction respectively for our model. Comparing the two versions of upgridded models it is evident in the vertical permeability distribution that the majority of the pure statistical model permeability information has been enhanced and therefore the model will deviate from the layer based method.

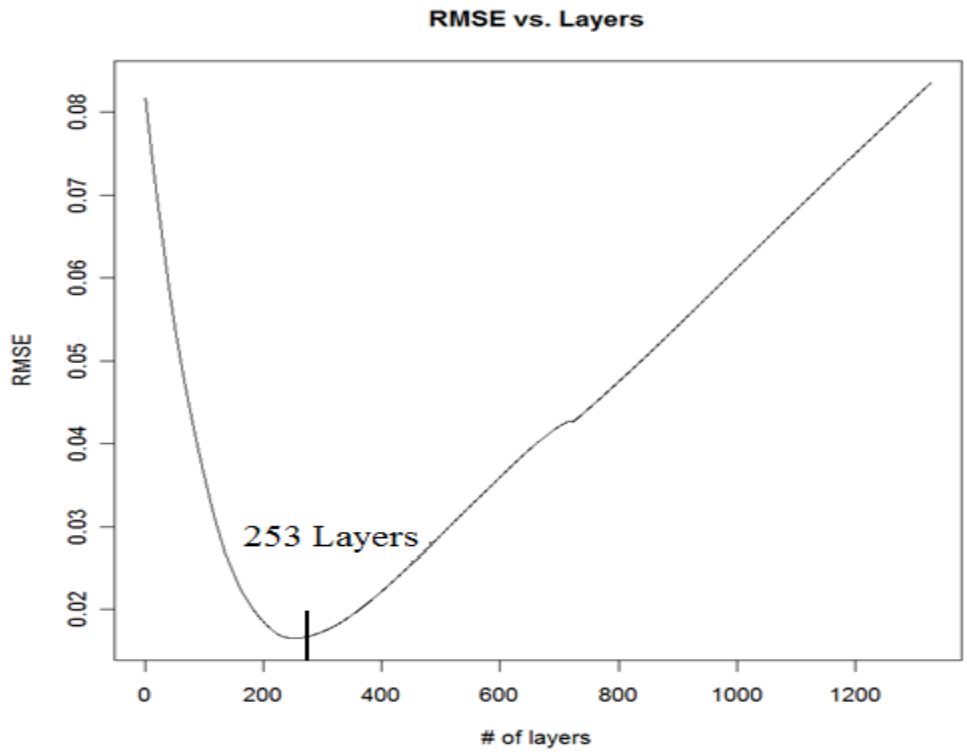

Figure 53 - 253 layer based statistical RMSE analysis.

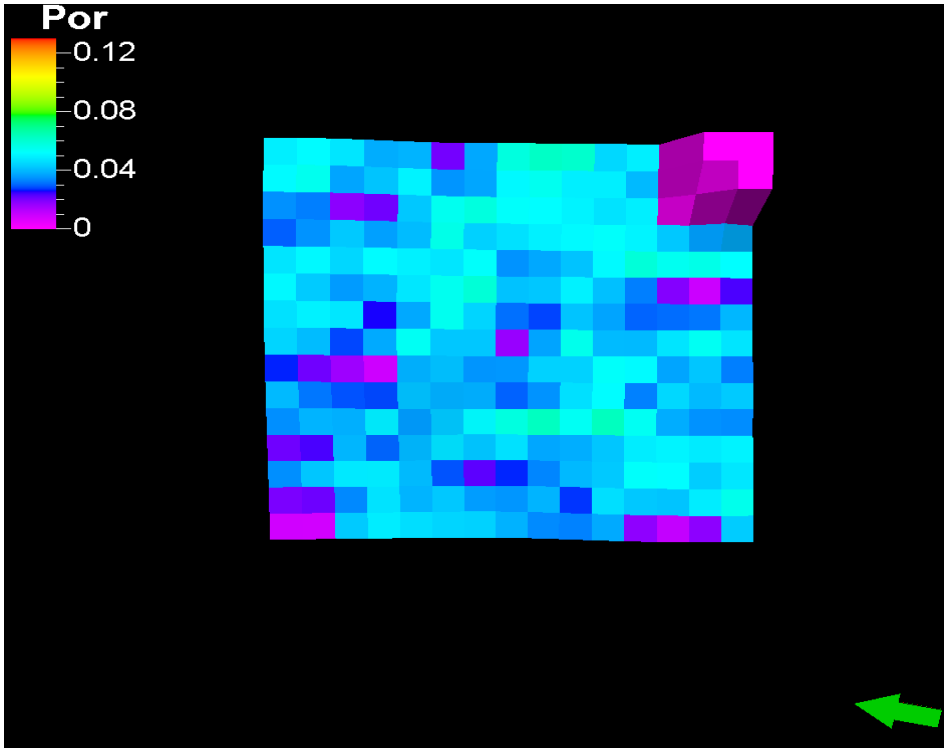

Figure 54- Areal porosity distribution for 253 layer model.

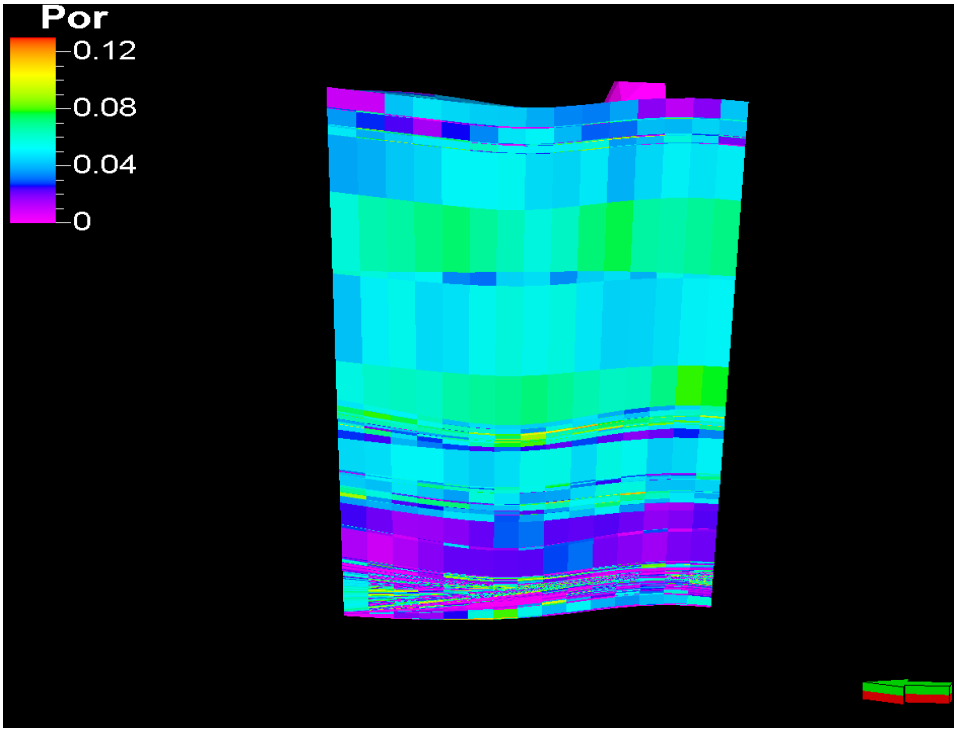

Figure 55- Vertical porosity distribution for 253 layer model.

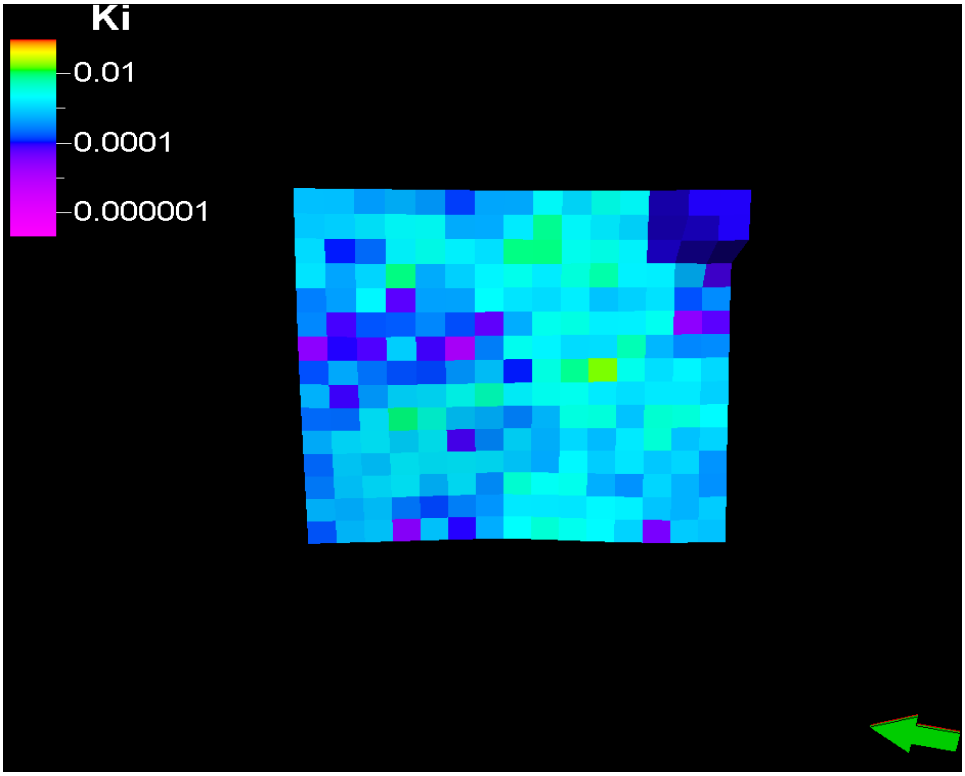

Figure 56 - Areal permeability distribution for 253 layer model.

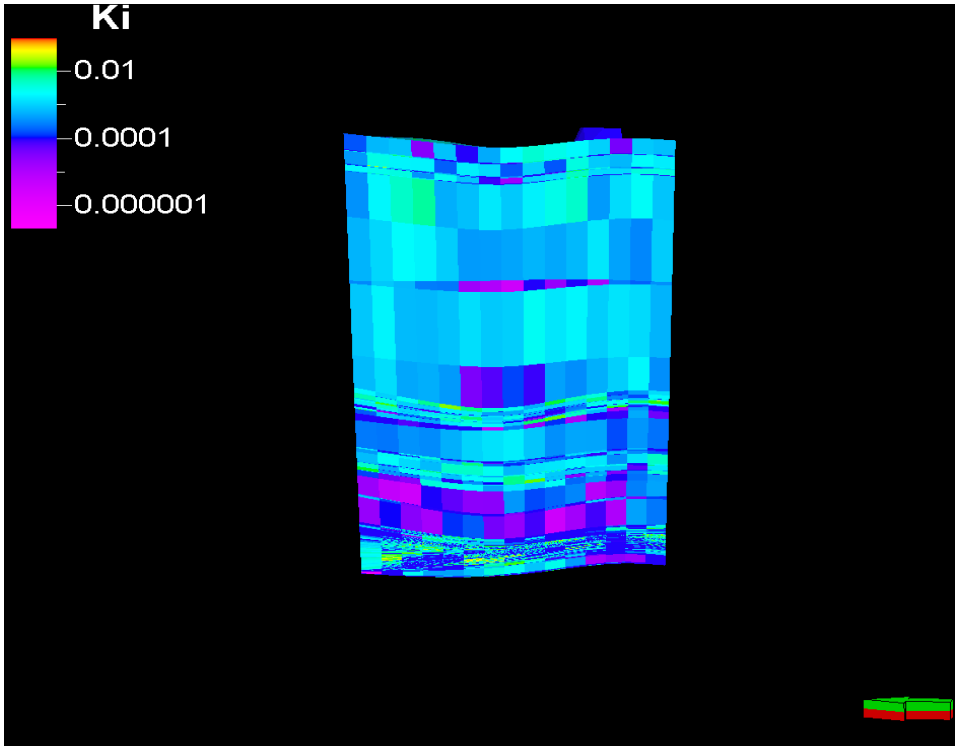

Figure 57- Vertical permeability distribution for 253 layer model.

6. CONCLUSIONS AND RECOMMENDATIONS

6.1 Conclusions

A non-uniform optimal upgridding approach was developed in C++ for both oil and gas reservoirs. The software is capable of using pure statistical analysis or using layer information to upgrid reservoir models. The algorithm has been applied to both an offshore channelized reservoir and a tight gas reservoir. Through the use of reservoir response including water cut, oil production, and bottomhole pressure we have validated our method in a channelized reservoir. Using visual grid comparisons we have shown that our method is capable of maintaining the individual zones that are present in reservoirs and are of importance when upgridding in a tight gas reservoir. An overview of the major conclusions from this work is summarized below.

1. A C++ program was developed that applies our algorithm for both oil and gas reservoirs with minimal user interaction that outputs new files to be used in simulation.
2. Our optimal upgridding approach creates a reservoir model that maximizes heterogeneity in the model after upgridding while minimizing the heterogeneity removed from the model due to upgridding.
3. Our non-uniform approach has shown to outperform uniform upgridding methods in preserving geological realism and simulating the fine scale model.
4. Layer based statistical optimization of the reservoir model is more accurate than the pure statistical based optimization method.

6.2 Recommendations

The next step in the upgridding process would be to recreate a new grid that is a true coarse model in the scale sense. Currently we only reassign properties to the fine scale grid base upon our algorithm. This process would create a new file that could be used directly from the runtime compilation in an eclipse data deck for simulation. This creates time savings during the simulation due to a reduced number of calculations.

When upgridding two layers, the merging of two rock types is possible even in layer based optimization and therefore the rock frontal velocity will be altered. Currently we do not recalculate the rock frontal velocity after two rock types have been merged. This is because we would be required to alter the relative permeability tables after each merging. By using the initial rock frontal velocities for each cell based upon the original bulk volume we do not need to update the relative permeability and fractional flow curves. The next step would be the recalculation of relative permeability and rock frontal velocity for each merging.

Finally the simulation of the tight gas reservoir application would further validate our algorithm. The initial modeling and upgridding has been completed for the reservoir. However, the fractures have not been applied to the reservoir through the use of transmissibility alterations in the flow direction. The cooperation of Schlumberger is still required to determine the half length of the fractures in each zone and their orientation. Until this is completed the comparison to a fine scale model is not useful because the flow of the reservoir will be severely altered by the fractures.

NOMENCLATURE

p	static property used for upgridding optimization
f'	Buckley-Leverett rock frontal velocity
k	permeability
ϕ	porosity
s_{wirr}	irreducible water saturation
B	heterogeneity preserved
NX	number of cells in x direction
NY	number of cells in y direction
NZ	number of cells in z direction
x	x direction iteration counter
y	y direction iteration counter
z	z direction iteration counter
n	cell bulk volume or ntg (net to gross)
p^c	transitional column average of static property
$\bar{p}$	fine scale column average of static property
W	heterogeneity removed
H	total heterogeneity
f_w	water fractional flow
k_{ro}	oil relative permeability
μ_o	oil viscosity
A	cross sectional area

q_t total flow rate

P_c capillary pressure

L length of flow

Δp pressure difference

α angle

k_{rw} water relative permeability

μ_w water viscosity

v velocity

q_i injection flow rate

$\frac{df_w}{ds_w}$ fractional flow slope used in determining rock frontal speed

$\frac{k_v}{k_h}$ vertical to horizontal permeability ratio

REFERENCES

Buckley, S.E. and Leverett, M.C. 1942. Mechanism of Fluid Displacement in Sands. *Trans.*, AIME **146**: 107-116.

Christie, M.A. and Blunt, M.J. 2001. Tenth SPE Comparative Solution Project: A Comparison of Upscaling Techniques. *SPEREE* **4** (4): 308-317. SPE-72469-PA. DOI: 10.2118/72469-PA.

Chawathé, A. and Taggart, I. 2004. Insights Into Upscaling Using 3D Streamlines. *SPEREE* **7** (4): 285-296. SPE-88846-PA. DOI: 10.2118/88846-PA.

Dake, L.P. 1978. Immiscible Displacement. In *Fundamentals of Reservoir Engineering*, ed. L.P. Dake, Chap. 10, 352-365. Amsterdam: Developments in Petroleum Science Series, Elsevier Scientific Publishing Co.

Durlofsky, L.J., Behrens, R.A., Jones, R.C., and Bernath, A. 1996. Scale Up of Heterogeneous Three Dimensional Reservoir Descriptions. *SPEJ* **1** (3): 313-326. SPE-30709-PA. DOI: 10.2118/30709-PA.

Efendiev, Y.R. and Durlofsky, L.J. 2004. Accurate Subgrid Models for Two-Phase Flow in Heterogeneous Reservoirs. *SPEJ* **9** (2): 219-226. SPE-88363-PA. DOI: 10.2118/88363-PA.

Fincham, A.E., Christensen, J.R., Barker, J.W., and Samier, P. 2004. Up-Gridding from Geological Model to Simulation Model: Review, Applications and Limitations. Paper SPE 90921 presented at the Annual Technical Conference and Exhibition, Houston, Texas, 26-29 September. DOI: 10.2118/90921-MS.

Gorell, S. and Bassett, R. 2001. Trends in Reservoir Simulation: Big Models, Scalable Models? Will you Please Make up Your Mind?. Paper SPE 71596 presented at the Annual Technical Conference and Exhibition, New Orleans, Louisiana, 30 September- 3 October. DOI: 10.2118/71596-MS.

Hohl, D., Jimenez, E.A., and Datta-Gupta, A. 2006. Field Experiences With History Matching an Offshore Turbiditic Reservoir Using Inverse Modeling. Paper SPE 101983 presented at the SPE Annual Technical Conference and Exhibition, San Antonio, Texas, 24-27 September. DOI: 10.2118/101983-MS.

King, M.J., Burn, K.S., Wang, P., Muralidharan, V., Alvarado, F., Ma, X., and Datta-Gupta, A. 2006. Optimal Coarsening of 3D Reservoir Models for Flow Simulation. *SPEREE* **24** (10): 317-334. SPE-95759-PA.

Kumar, A., Farmer, C.L., Jerauld, G.R., and Li, D. 1997. Efficient Upscaling from Cores to Simulation Models. Paper SPE 38744 presented at the SPE Annual Technical Conference and Exhibition, San Antonio, Texas, 5-8 October. DOI: 10.2118/38744-MS.

Li, D. and Beckner, B. 2000. Optimal Uplayering for Scaleup of Multimillion-Cell Geologic Models. Paper SPE 62927 presented at the SPE Annual Technical Conference and Exhibition, Dallas, Texas, 1-4 October. DOI: 10.2118/62927-MS.

Milliken, W.J., Levy, M., Strebelle, S., and Zhang Y. 2008. The Effect of Geologic Parameters and Uncertainties on Subsurface Flow: Deepwater Depositional Systems. Paper SPE 114099 presented at the SPE Western Regional and Pacific Section AAPG Joint Meeting, Bakersfield, California, 31 March – 2 April. DOI: 10.2118/114099-MS.

Nair, C.V.G. and Al-Maraghi, E. 2006. A Practical Approach in Building Upscaled Simulation Model for a Large Middle East Carbonate Reservoir Having Long Production History. Paper SPE 100270 presented at the SPE Europec/EAGE Annual Conference and Exhibition, Vienna, Austria, 12-15 June. DOI: 10.2118/100270-MS.

Osako, I. and Datta-Gupta, A. 2007. A Compositional Streamline Formulation With Compressibility Effects. Paper SPE 106148 presented at the SPE Reservoir Simulation Symposium, Houston, Texas, 26-28 February. DOI: 10.2118/106148-MS.

Qi, D. and Hesketh, T. 2004. Quantitative Evaluation of Information Loss in Reservoir Upscaling. Paper SPE 87035 presented at the SPE Asia Pacific Conference on Integrated Modeling for Asset Management, Kuala Lumpur, Malaysia, 29-30 March. DOI: 10.2118/87035-MS.

Sablok, R. and Aziz, K. 2005. Upscaling and Discretization Errors in Reservoir Simulation. Paper SPE 93372 presented at the Reservoir Simulation Symposium, Houston, Texas, 31 January – 2 February. DOI: 10.2118/93372-MS.

Stern, D. and Dawson, A.G. 1999. A Technique for Generating Reservoir Simulation Grids to Preserve Geologic Heterogeneity. Paper SPE 51942 presented at the Reservoir Simulation Symposium, Houston, Texas, 14-17 February. DOI: 10.2118/51942-MS.

Testerman, J.D. 1962. A Statistical Reservoir-Zonation Technique. *JPT* **14** (8): 889-893. SPE- 286-PA. DOI: 10.2118/286-PA.

Wang, K., Sepehrnoori, K., and Killough, J.E. 2005. Ultrafine-Scale Validation of Upscaling Techniques. Paper SPE 95774 presented at the Annual Technical Conference and Exhibition, Dallas, Texas, 9-12 October. DOI: 10.2118/95774-MS.

Wu, X.H., Stone, M.T., Parashkevov, R.R., Stern, D., and Lyons, S.L. 2007. Reservoir Modeling With Global Scaleup. Paper SPE 105237 presented at the Middle East Oil and Gas Show, Kingdom of Bahrain, 11-14 March. DOI: 10.2118/105237-MS.

Zhang, P., Pickup, G., and Christie, M. 2006. A New Method for Accurate and Practical Upscaling in Highly Heterogeneous Reservoir Models. Paper SPE 103760 presented at the International Oil and Gas Conference, Beijing, China, 5-7 December. DOI: 10.2118/103760-MS.

APPENDIX A

SOFTWARE USERS MANUAL

The software is capable of upgridding both oil and gas reservoirs. The software will ask the user if the reservoir is oil or gas. If it is an oil reservoir the user enters the character ‘O’ or ‘o’ into our software during runtime when prompted. If it is a gas reservoir then the user enters the character ‘G’ or ‘g’ into our software during runtime when prompted. Our software and algorithm is for two phase reservoirs. The oil reservoir case assumes water as the second phase and uses Buckley-Leverett calculations to determine the rock frontal speed for each distinct rock in the model. This frontal speed is used in the static property, *p*, which is used for determining the minimum variance in the algorithm. Gas cases do not use the rock frontal speed in the algorithm. We assume that the other phase is water at the irreducible saturation so that the permeability can be used in our static property *p* or that the permeability is the effective gas permeability. The software uses vectors that start with index 0 for all properties read into the program. For example a data set read into a vector named *data* that consists of 350 values will begin with *data*(0) and end in *data*(349). Our software also alters nulled reservoir values that are represented as -999 and replaces with the value 0 in all information that is read into the program. The second option that is available in our software is upgridding based upon pure statistical calculations or upgridding based upon both layer (zone) information and statistical information. The user will enter either (S) for pure statistical optimization or (L) for layer based statistical optimization. The software will then ask the user how many layers they would like the program to terminate. The first time the user applies our

program the number of layers to be terminated at depends upon the type of optimization. If the upgridding is to be performed on a pure statistical basis (S) then the user should enter 2 when asked how many layers should remain at the end of the upgridding. If the upgridding is to be performed on a layer based statistical (L) approach then the number of remaining layers **must** be equal to the number of layers in the reservoir model or the program will terminate in failure. This applies only for the first run of our program. After we initially run the program we then take our results in layerwt.txt which is output by the program and run the R statistical software as explained in the following appendix. Once we have run the R statistical software we have the optimal number of layers to be used in our second running of the algorithm. This value is to be input into the software when prompted for how many remaining layers regardless of the type of upgridding is performed.

After determining if the reservoir is oil or gas and what type of upgridding to perform the software will search the folder that the program was launched in to find the porosity, permeability, height, bulk volume (or ntg), oil viscosity, water viscosity, relative permeability tables, and rock number for oil reservoirs. If it is a gas reservoir the program only reads in the porosity, permeability, height, bulk volume (or ntg) to perform the upgridding because the rock type and relative permeability curves are not needed in our algorithm. It is important to note that all relative permeability tables that are read into the program before chord slope enhancements must have the second saturation value equal to the irreducible water saturation. The program will take the relative

permeability tables that are provided by the user and recreate the relative permeability curves using 100 points using equation A-1.

$$k_{r(new)} = \frac{k_r(i+1) - k_r(i)}{s_w(i+1) - s_w(i)} * \left(s_{w(new)} - s_w(i)\right) + k_{r(old)} \qquad \text{A-1}$$

The program output will provide an error if any of the information is missing and the program cannot continue. Based upon the reservoir type the vector *localvelocity* will be filled with the static property, *p*, which was defined in the variance analysis portion of this thesis. Our algorithm then calculates a surface average for each layer in our model equal to equation A-2

$$psurfave = \frac{\sum_i bulkvol}{\sum_i \frac{bulkvol}{localvelocity}} \qquad \text{A-2}$$

This value is used in the algorithm after each layer is merged. The software then takes an average of the merged layers *psurfave* which is labeled as *kc* in the algorithm. This value can be watched in the runtime if the user would like to spot check how our algorithm is merging the layers on a layer average perspective. This is the only use for this value in our algorithm. We then calculate the column average for each column in the model using equation A-3.

$$colpave = \frac{\sum_j bulkvol}{\sum_j \frac{bulkvol}{localvelocity}} \qquad \text{A-3}$$

The software creates vectors for the active layers known as *btwo*, a between cell variance known as *bw*, a within cell variance known as *wt*, a residual known as *resv*, and simulation layers remaining known as *siml*. Before the software enters the main loop we calculate the total model variance using the equation 2.1.

The next step is to enter the main loop of our program that finds two layers to merge. The first active layer is found in the *btwo* vector, active layers are assigned the value 1 and inactive are assigned 0, and we loop until the index of the second active layer is found. Once these locations are found we calculate a new property to determine the residual between the two layers. Equation A-4 is the formula for determining the residual. This is our column based analysis as the 1 and 2 subscripts denote the vertical layers that are being compared in each areal cell. This is a bulk weighted average times the squared difference between the two layers static properties known as *localvelocity*. The calculated *resi* is then summed up in the areal direction to provide the total residual between the active layers.

$$resi = \frac{(bulkvol_1 * bulkvol_2)}{(bulkvol_1 + bulkvol_2)} * (localvelocity_1 - localvelocity_2)^2 \qquad \text{A-4}$$

The software loops through the entire model and calculate residuals for each set of neighboring active layers. We then search for the minimum residual in the vector and use the corresponding two layers as the layers to be merged. After two layers have been merged, we then reassign the lower layer to be inactive by assigning the value of zero into the *btwo* vector at the lower layer index location.

The software then calculates the within cell variation and between cell variation using the respective equations located in the variance analysis section. The software loops until the total number of layers is equal to 2 or the terminating layer amount if layer based optimization is chosen by the user during runtime and then a switch tells the software to exit the merging loop. After each merging the permeability and porosity are stored for the new layer using the following equation A-5 and equation A-6. These

values are stored and then finally output to a .GRDECL file for simulation after the required number of layers to be merged criteria is met.

$$phi = \frac{(bulkvol_1 * phi_1)+(bulkvol_2 * phi_2)}{(bulkvol_1+bulkvol_2)} \quad \text{A-5}$$

$$perm = \frac{(height_1 * perm_1)+(height_2 * perm_2)}{(height_1+height_2)} \quad \text{A-6}$$

Finally the program will output a file called New_Layering.txt in this file the merged layers are output in a user friendly format. This format will show the user which layers have been merged in the format shown in the following manner:

```
1-38
39-40
41-41
42-71
72-72
73-74
75-75
76-89
90-90
91-91
92-203
```

This output is telling the user that layers 1 through 38 have been merged followed by layers 39 through 40. It is important to know that the output shows 41-41 meaning that layer 41 has not been merged in our algorithm.

APPENDIX B

R STATISTICAL SOFTWARE

The optimal number of layers are determined using a statistical software known as R. Xianlin Ma has written a script that uses the layer information and amount of heterogeneity removed (W) to determine the optimal number of layers.

Regression mean square error (RMSE) analysis is performed by applying two linear regressions to the removed heterogeneity information. We will call the two linear regressions by the names Leftreg and Rightreg. For example if there are 50 data points then the Rightreg will start by applying a linear regression to the last two data points and the Leftreg will apply a linear regression to the remaining 48 points starting from the first data point. We then add a single data point to the Rightreg regression and similarly remove a data point from the Leftreg linear regression. In our example this creates a 3 point data set for the Rightreg and 47 data point set for the Leftreg linear regressions. We continue this process until the Leftreg data set has 2 data points and the Rightreg data set has 48 data points. We calculate the data set weighted residual for both regressions at each iteration and use their summation as the RSME used in our plot versus the number of layers.

The following is the script that has been developed to determine the optimal number of layers in R. The first line reads the file in the working directory labeled as layerwt.txt into the program as dat. A plot is produced that compares RMSE vs. layers and can be visually analyzed to determine the optimal number of layers. After running the script the program will output the RMSE information in a file labeled as RSME.out which can be

opened in a text editor or excel to determine the precise location of the minimum if visual inspection of the plot is not satisfactory.

```
dat <- read.table("layerwt.txt",head=F)
# use wt to find optimal layers
b <- dat$V2
nb <- length(b)
b1 <- b[nb:1]
#remove the first point
b1 <- b1[-1]
nb <- length(b1)
a <- 2:(nb+1)
#a <- 1:nb
k<-0
rm.a <- rep(-1,90)
for (c in 3: (nb-3) ) {
  l.y <- b1[1:c]
  l.x <- a[1:c]
  lc <- lm(l.y~l.x)
  rm.lc <- sqrt( sum(lc$residual^2)/c )
  r.y <- b1[(c+1):nb]
  r.x <- a[(c+1):nb]
  rc <- lm(r.y ~ r.x)
  rm.rc <- sqrt( sum(rc$residual^2)/(nb-c) )
  k <- k +1
  rm.a[k] <- ((c-1)*rm.lc + (nb-c)*rm.rc)/nb
}
plot(rm.a[rm.a>0],type="l",main="RMSE vs. Layers",xlab="# of
layers",ylab="RMSE")

write.table(rm.a[rm.a>0],"rmse.out",row.names = F, col.names = F, quote
= F)
```

VITA

Matthew Brandon Talbert received his Bachelor of Science degree in petroleum engineering from Texas A&M University at College Station in 2006. He entered the petroleum engineering graduate program at Texas A&M University in September 2006 and received his Master of Science degree in August 2008. His research interests include reservoir simulation and reservoir engineering.

Mr. Talbert may be reached at 3116 TAMU – 507 Richardson Bldg., College Station, TX. 77843-3116. His email is talbert.matt@gmail.com.